DOI:10.14753/SE.2015.1712

The possible role of estradiol and estrogen receptor alpha in TGF-β induced type II epithelial-mesenchymal transition and the following regeneration in mesenteric mesothelial cells

PhD thesis

dr. Petra Balogh MD

Doctoral School of Molecular Medicine

Semmelweis University

Supervisor: Dr. Anna L. Kiss C.Sc

Official reviewers:
Dr. András Kiss Ph.D
Dr. Kinga Molnár Ph.D

Head of the Final Examination Committee:
Dr. László Tretter D.Sc

Members of the Final Examination Committee:
Dr. Zsuzsanna Darvas Ph.D
Dr. Péter Löw Ph.D

Budapest, 2014

DOI:10.14753/SE.2015.1712

Table of Contents

DOI:10.14753/SE.2015.1712

DOI:10.14753/SE.2015.1712

1. List of Abbreviations

4A	androstendione
AMPK	AMP-activated protein kinase
BMP	bone morphogenetic protein
CD63	cluster of differentiation 63
DHEA	dehidroepiandrosterone
DNA	deoxyribonucleic acid
E2	estradiol
E2-S	estradiol-sulfate
EDTA	ethylenediaminetetraacetic acid disodium salt
EEA1	early endosome antigene-1
EGF	epidermal growth factor
EMT	epithelial-mesenchymal transiton
ER –α	estrogen-receptor alpha
ERK	extracellular signal-regulated kinase
ESCRT	endosomal sorting complexes required for transport
EST	estradiol sulfate
FGF	fibroblast growth factor
FGF	fibroblast growth factor
FYVE	zink finger domain named after the four cysteine.rich proteins:Fab1, YOTB, Vac1, EEA1
GDF	growth differentiation factor
GDNF	glial cell-line derived neurotrophic factor
GPI	glycophosphatidylinositol
GPR30	G protein coupled receptor 30
IGF	insulin-like growth factor
IL	interleukin
ILV	intraluminal vesicle
JNK	c-Jun N-terminal kinase
LC3	microtubule-associated protein light chain 3
MAPK	mitogen-activated protein kinase

DOI:10.14753/SE.2015.1712

MH	Mad Homology
mRNA	messenger ribonucleic acid
mTOR	mammalian target of rapamycin
MVB	multivesicular body
NES	nuclear export signal
NLS	nuclear localization signal
NPS	nuclear pore signal
PI3K	phosphatidylinozitol-3-kinase
PKC	protein kinase C
qRT-PCR	quantitative real-time polymerase chain reaction
SARA	Smad anchored for receptor activation
Smad	Sma and Mad homology domains
T	testosteron
TGF-β	transforming growth factor beta
TNF	tumor necrosis factor

DOI:10.14753/SE.2015.1712

2. Introduction

2.1 Epithelial-mesenchymal transition

Epithelial-mesenchymal transition (EMT) is a biological process that allows a polarized epithelial cell to undergo several biochemical and morphological changes to obtain a mesenchymal phenotype (Kalluri&Weinberg 2009). Epithelial cells typically form an uniform array, often a monolayer. The cells are adhered to each other via cell-cell junctions providing a tight connection between the neighbouring cells. Epithelial cells furthermore are polarized meaning that apical and basolateral surfaces are responsible for different cellular functions. Mesenchymal cells, in contrast are elongated, spindle-shaped, apolar cells and are capable of locomotion as they are lacking intercellular adhesions (Lee et al 2006). This capacity for plasticity, the process of EMT was first described by Elisabeth Hay who also depicted the basic differences of the cellular actions observed during embryogenesis and tumorigenesis (Hay 2005). Since then three subtypes of EMTs have been distinguished with different functional consequences. Besides epithelial-mesenchymal transition during embryogenesis (type I) and tumorigenesis (type III), type II EMT is associated with wound healing, tissue regeneration and organ fibrosis (Sodek et al 2012, Yanez Mó et al 2003). It has been demonstrated that upon inflammation many cells (monocytes/macropaghes, fibroblasts) can trigger type II EMT through secretion of growth factors such as transforming growth factor-beta (TGF-β) or epidermal growth factor (EGF). Most prominent among these cells are the macrophages and activated resident fibroblasts that accumulate at the site of injury and release these growth factors (Kalluri&Weinberg 2009, Lee et al 2006, Strutz et al 2002) (Fig. 1). TGF-β was first described to induce EMT via the canonical Smad 2/3-dependent pathway and meanwhile it became evident that the cellular actions of the cytokine can be modulated by other Smad-independent signaling pathways like MAP kinase pathways (Zavadil&Böttinger 2005, Derynck&Zhang 2003, Massagué 1998).

DOI:10.14753/SE.2015.1712

2.1.1 TGF-β superfamily

TGF-β superfamily consists of numerous groups of cytokins that regulate a diverse set of cellular processes. Besides the TGF-β isoforms (TGF-β_1, TGF-β_2 and TGF-β_3), further members of the family include the bone morphogenetic proteins (BMP), inhibin, myostatin, Nodal, GDF, GDNF, MIS (Müllerian Inhibiting Substance), each with different roles in cell differentiation, apoptosis, cell migration and adhesion during embryogenesis and in adult tissues (Massagué 1998). TGF-β has also dual role depending on the cell type and the environment. While it is able to suppress cell growth in epithelial and hemopoetic cells by inducing G_1 arrest, it also initiates cell proliferation and differentiation in mesenchymal cells. The cellular processes that regulate the morphological plasticity of a cell and result in phenotypic change is known as epithelial-mesenchymal transition (EMT) (Shook&Keller 2003). The universal role of TGF-β in the different types of EMTs is unambigous as well as the biochemistry of the signaling is well characterized. It is less clear, however in which cellular/cytoplasmic compartments the molecules along the downstream pathway are accommodated and how their localization changes with the dynamics of the signaling. Another question of great interest is whether different compartments can be involved in regulating the pathway and if so, whether they can promote or suppress the signaling events?

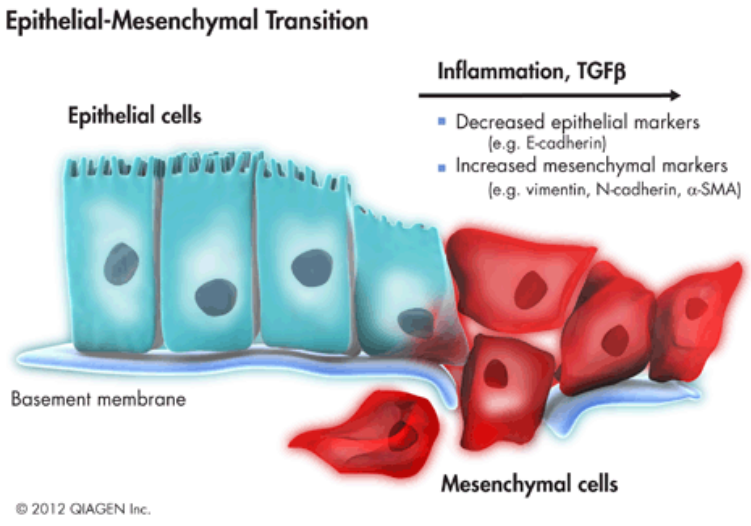

Figure 1. Inflammation and growth factors like TGF-β promote mesenchymal transition. Epithelial-mesenchymal transition takes place during development, and is also proposed to play a role in cancer invasion and generation of myofibroblasts that contribute to fibrosis. In response to injury, inflammatory cells and activated fibroblasts produce growth factors such as TGF-β and FGF-2, as well as matrix metalloproteinases and chemokines. TGF-β and other factors trigger signaling cascades in epithelial cells that lead to a change from an epithelial to a mesenchymal phenotype (Source: Kalluri&Weinberg 2009, Strutz et al 2002).

2.1.2 The TGF-β signaling events

TGF-β, the prototype of the family, signals through its cell surface serine/threonin kinase receptors. Functionally and structurally type I and type II TGF-β receptors (TβR-I, TβRII) can be distinguished. The type II receptor is considered a constitutively active kinase (activated by autophosphorylation) while type I receptor contains a special GS domain the phosphorylation of which leads to the activation of the receptor. In the prototypic TGF-β pathway, ligand binds to type II receptor and induces the formation of a heterotetrameric receptor complex within which TβR-II transphosphorylates and activates the type I receptor and the activated TβR-I initiates the Smad signal transduction pathway (Shi&Massagué 2003, Massagué 1998, Wrana et al 1994).

The Smad proteins are subgrouped based on their structural and functional differences. The i) receptor-regulated (R)-Smad proteins are Smad 2,3 that are the only substrates for type I receptor kinases while further members of this group include Smad 1,5,8, that are phosphorylated by the activated BMP receptors. After phosphorylation, thus activation, the R-Smads associate with ii) common mediator (Co)-Smad protein, Smad4. They form oligomeric complexes and are transported to the nucleus to regulate the transcription of target genes together with other nuclear cofactors. The members of the third class of Smads act as negative regulators of the signaling pathway: iii) inhibitory (I)-Smads include Smad6 and Smad7 proteins (Shi&Massagué 2003, Moustakas et al 2001, Zhang et al 2001).

Recent findings have demonstrated that accessory proteins interact with type I, type II receptors and Smad proteins (Moustakas et al 2001). An example is SARA (Smad

anchor for receptor activation) that facilitates the association of R-Smads with TGF-β receptor at the plasma membrane, though it is predominantly localized and bound to phosphatidylinositol 3-phosphate (PtdIns3P) rich early endosomes (Di Guglielmo et al 2003, Tsukazaki et al 1998). Furthermore, some data suggest that SARA can interact with cell surface TβRs and in this way protects the complex from degradation (Chen 2009, Chen at al 2007, Gillooly et al 2001, Itoh et al 2002).

Ligand binding to its cell surface receptors means not only the beginning of the signaling events through Smads, but also triggers internalization of both ligand and receptors (Chen 2009, Chen at al 2007, Le Roy&Wrana 2005, Itoh et al 2002, Gillooly et al 2001). The receptor internalization is required for the initiation of downstream signaling. There are two main endocytic pathways through which the TGF-β ligand-receptor complex can be internalized (Di Guglielmo et al 2003). One of them is the well-characterized clathrin-mediated endocytosis and a less clear pathway is the lipid/caveola-mediated endocytosis. Both types of pathways are used for the internalization of TβRs. It is already clear that via different internalization routes cells can control the number of surface-receptors and this is crucial for regulating the signaling, receptor turnover, the magnitude and duration of the events (Chen 2009).

2.1.3 Clathrin-mediated endocytosis enhances the signaling

Internalization of most cell surface receptors is mediated by short specific sequences in their cytoplasmic domain. Tyrosine-containing sequences and di-leucin-based motifs function as internalization signals for clathrin-dependent endocytosis. These sequences can directly bind to the endocytic machinery and play important role in cargo enrichment on the clathrin-coated pit as well as in vesicle formation (Bonifacino&Traub 2003, Bonifacino&Lippincott-Schwartz 2003). Such internalization signals have also been identified in TGFβ receptors. Both TβRI and TβRII appear to be rapidly internalized upon ligand binding. After receptor-ligand internalization in clathrin coated vesicles, the complex is targeted into EEA1 (early endosome antigene-1) positive endosomes. These compartments promote the signal transduction by recruiting the FYVE domain-containing proteins (like SARA). The C-terminal phosphorylation of R-

Smads bounded to endosomal membranes leads to their dissociation from both SARA and receptor (Di Guglielmo et al 2003, Hayes at al 2002, Penheiter et al 2002). Afterwards the phosphorylated R-Smads can bind to Smad4 (Xu et al 2000) forming the oligomeric complex that can enter the nucleus to regulate target genes in association with other coactivators and corepressors. It is important to emphasize that although clathrin-mediated endocytosis of TβRs can enhance Smad-mediated TGFβ signaling, it is still debated whether this process is required for the signaling (Hayes et al 2002, Penheiter et al 2002). Thus, early endosomes (EE) are important not only in the sorting of internalized cargo proteins and receptors but by providing a special microenvironment through recruiting the signaling molecules (Hayes et al 2002), they presumably play role in defining the activity of signaling events as well.

After dissociation, TGF-β receptors can either recycle back to the plasma membrane in recycling endosomes (Mitchell et al 2004) or be degraded in the downstream endosomal compartments.

The shuttling of TGFβ-induced Smad complexes between the cytoplasm and the nucleus is strictly regulated. The R-Smad and Co-Smad proteins have conserved Mad-homology 1 (MH1) and MH2 domains connected by a linker domain, while the I-Smads are lack a distinct MH1 domain. The R-Smads and Co-Smad have a nuclear localization sequence (NLS) in their Mad-homology 1 (MH1) domain while their MH2 domain contains nuclear export signal (NES) and nuclear pore signal (NPS) as well (Heldin&Moustakas 2012) (Fig. 2). Phosphorylated Smad3 was shown to interact with importin-β1 of the nuclear pore and enters into the nucleus in a GTPase dependent manner (Xiao et al 2003, Kurisaki et al 2001).

DOI:10.14753/SE.2015.1712

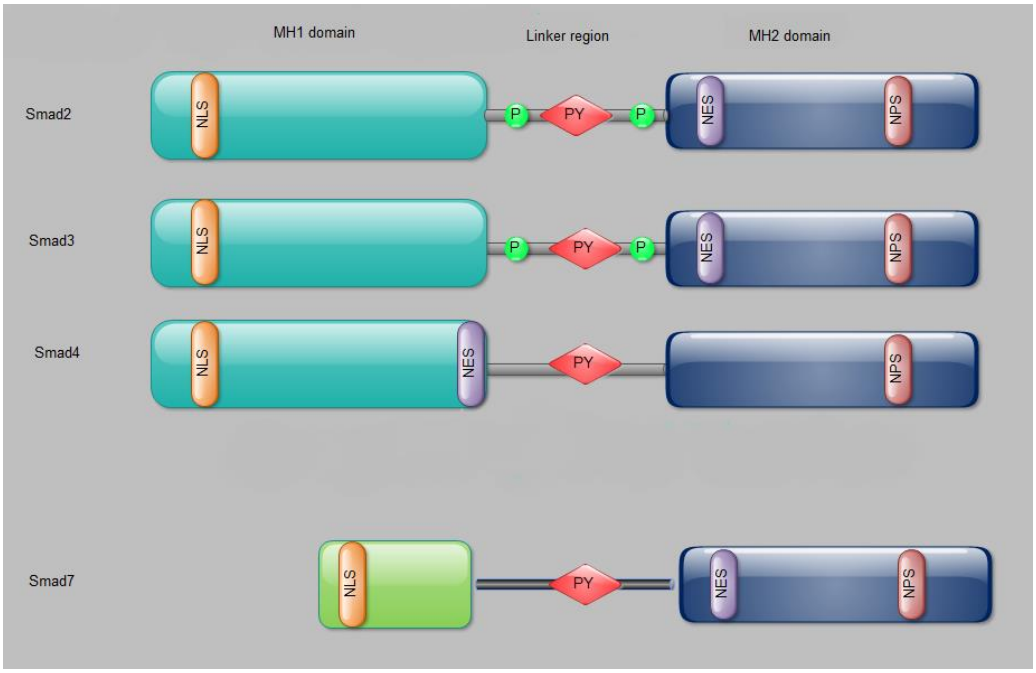

Figure 2. Functional domains of Smad proteins. The R-Smad (Smad2/3) and Co-Smad (Smad4) proteins have conserved Mad-homology 1 (MH1) and MH2 domains connected by a linker domain, while the I-Smad (Smad7) lacks a distinct MH1 domain. The MH1 domain contains DNA-binding site (except for Smad2) and nuclear localization signal (NLS) and mediates interactions with different transcription factors to stabilize the nuclear Smad complex. MH2 domain is higly conserved among all Smads and is responsible for receptor interaction, the nucleocytoplasmic shuttling of Smad proteins (NPS, NES) and also mediates the formation of Smad oligomer complexes and the interaction of other proteins such as SARA. The linker region contains phosphorylation sites allowing crosstalks with other signaling pathways and binds ubiquitin ligases (Smurf proteins) via the PY motif. (Source: Balogh et al 2013).

2.1.4 Caveola-mediated endocytosis attenuates TGF-β signaling

Another internalization route into the cell is via caveolin-1 positive vesicles. It is known that TβRs are accommodated in caveolin-1 containing lipid rafts of the plasma membrane and use this internalization route as well. Caveolae are small omega or flask-shape plasma membrane invaginations that play important role in many cellular functions including endocytosis, signal transduction, cellular growth control and apoptotic cell death. The main protein components of caveolae are the scaffolding

proteins termed caveolin-1,-2,-3 (Couet et al 1997, Lisanti et al 1994). Complex events lie behind the regulation of the internalization pathway through caveolae and the intermediate compartments are still less clear. Earlier data showed that caveolae internalize into the cell, and form so-called caveosomes that were supposed not to communicate with other cellular compartments. According to this idea caveosomes would represent an individual cytosolic compartment the content of which may avoid lysosomal degradation (Nicols 2002, Pelkmans et al 2001). Recent data, however, have shown that caveolin-positive vesicles can also associate with early endosomes (Parton&Simons 2007) or might continuously remain in connection with the plasma membrane (Kiss&Botos 2009). Meanwhile, however the terminology ’caveosome’ as a distinct cellular compartment was repealed (Parton&Howes 2010). Caveolar endocytosis presumably provides another possible way for sequestering receptors (Le Roy&Wrana 2005). Several lines of evidence support the idea that receptor-ligand internalization via the (non-classical) caveolar pathway turns off the TGFβ signaling events by targeting the receptor-ligand complex to lysosomal and/or proteasomal degradation (Chen 2009, Le Roy&Wrana 2005, Di Guglielmo et al 2003). This receptor degradation plays an important role in controlling the amount of receptors on the plasma membrane. The possible pathways targeting the signaling molecules towards degradation are not entirely known and most of the papers avoid the detailed discussion of these routes. The inhibitory Smad (I-Smad), Smad7 is one of the main regulator in the degradative events. I-Smad inhibits TGFβ signaling through multiple mechanisms as a decoy substrate forming a stable complex with receptors to prevent recruitment of R-Smads (Nakao et al 1997, Hayashi et al 1997) and also disrupts the functional Smad-DNA complex formation (Zhang et al 2007). Smad7 exerts its negative effects at the level of the plasma membrane by competing with R-Smads for the receptor and also by recruiting the E3 ubiquitin ligase Smurf1/2 proteins to the active TβRs (Ebisawa et al 2001, Kavsak et al 2000, Nakao et al 1997) to promote receptor ubiquitination and degradation (Heldin&Moustakas 2012). (Smad7 has a putative NLS in its N-terminal region and resides in the nucleus in non-stimulated cells. In response to TGFβ stimulus, Smad7 leaves the nucleus in complex with the ubiquitin ligases, Smurf1/2 (Heldin&Moustakas 2012, Ebisawa et al 2001, Kavsak et al 2000, Itoh et al 1998). The interaction of Smad7 and Smurf proteins with activated TβRs targets the complex to

lipid rafts/caveolae and in this way the caveola-mediated endocytosis could promote receptor turnover and the termination of signaling (Di Guglielmo et al 2003).

TGFβ receptors after receptor ubiquitination have been shown to be degraded by both lysosomal and proteasomal machineries (Kowanetz et al 2008, Kavsak et al 2000). Though limited data are available on factors controlling the proteasomal degradation of TGFβ receptors. Recent data showed that a GPI-anchored protein, CD109 functions as a TGFβ co-receptor, associates with caveolin-1, promotes the caveolar localization of the TGFβ receptors and might regulate its proteasomal degradation (Bizet et al 2011). However, it is not clear how the caveolar endocytic machinery can drive receptors to the proteasomal pathway.

Besides TβRs, the stability of Smad proteins and caveolin is also controlled by ubiquitination suggesting the regulatory role of different ubiquitination signals. While poliubiquitination is a sign that directs the cargos to proteasomes, mono/multiubiquitination is a signal for the entry of proteins via the endocytic pathways. Thus, ubiquitination, indeed plays essential role both in signal transduction and also to determine the way of degradation towards proteasomes or towards multivescular body/late endosomes (Mukhopadhyay&Riezman 2007, Ciechanover 2005).

2.1.5 Multivesicular body formation

The lysosomal degradation of internalized cargos via caveolar endocytosis includes multivesicular body (MVB) formation and the early endosomes are the clue compartments of this process as well. Internalized cargo proteins are targeted first to early endosomes (Hayer et al 2010) indicating that MVB formation starts at the level of this cellular compartment. MVBs are formed when limiting membrane of endosomes invaginates and buds into the lumen of the organelles. (Gruenberg&Maxfield 1995, Felder et al 1990). A subset of membrane proteins within the limiting membrane of the endosomes are sorted into these invaginating vesicles and this sorting requires the inclusion of a 350kDa complex, called ESCRT-1 (endosomal sorting complexes required for transport). The membrane of early endosome (EE) contains the ESCRT complex that recognizes and binds ubiquitinated cargos and initiates the transport of the

cargos to late endosomes/multivesicular bodies. MVB sorting into intraluminal vesicles (ILV) and the subsequent lysosomal degradation of cell surface receptors is therefore a critical mechanism for regulating the signaling events (Katzmann et al 2001). Furthermore, the asymmetric compositon of the limiting membrane of these endosomal compartments presumably provide a platform for generating unique signals as well (Hanson&Cashikar 2012) (Fig. 3). Hence, early endosomes play a central role not only promoting the TGF-β pathway, but it is likely to be important intermediate cytosolic compartments that help to attenuate the signaling as well.

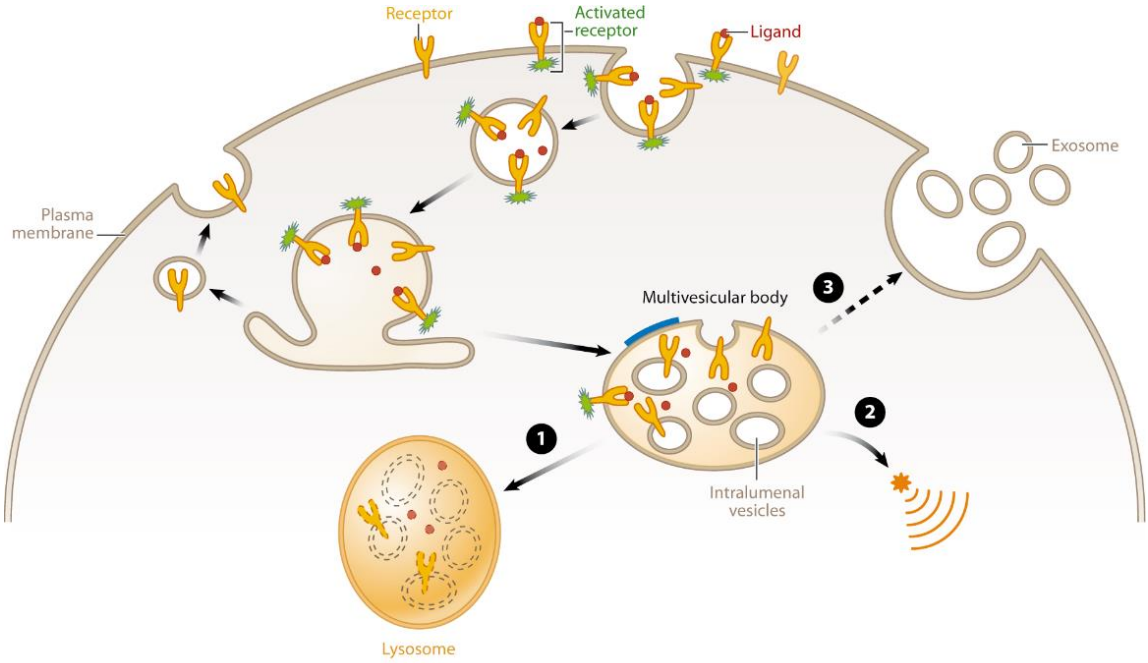

Figure 3. Multivesicular body (MVB) function. Schematic diagram showing the general functions of multivesicular bodies. Receptors (yellow) are activated (denoted in green) upon binding to their ligands (red) and then enter the cell by endocytosis. Receptors may be recycled back to the plasma membrane or may be targeted to intralumenal vesicles (ILVs) in the MVB. Decreasing pH in the early endosome, MVB and lysosome are indicated by different shades of orange. The thick blue line on the MVB limiting membrane indicates the characteristic flat bilayered coat. Fusion of MVBs with lysosomes leads to degradation of ILV content (1). MVBs also provide a platform for the generation of unique signals (2). Finally, MVBs can fuse with the plasma membrane to release ILVs in the form of exosomes (3). (Source: Hanson&Cashikar 2012)

DOI:10.14753/SE.2015.1712

2.1.6 Non-Smad signaling pathway

Besides the (canonical) Smad-pathway, TGFβ activates other non-Smad signaling pathways such as ERK, JNK, p38 MAP kinase pathways in a cell-specific and context-dependent manner. MAPK pathways help and complete the process of TGFβ induced epithelial-mesenchymal transition, although the mechanism by which TGFβ activates these pathways and their biological consequences are poorly characterized (Moustakas&Heldin 2005, Derynck&Zhang 2003). MAPK cascade is composed of several protein kinases that specifically phosphorylate and activate each other. The elements of the cascade are organized in levels that are termed MAP kinase kinase kinase (MAPKKK), MAP kinase kinase (MAPKK) and MAP kinase (MAPK). The activation of MAPK leads to its translocation to the nucleus where MAPK phosphorylates and activates its targets, e.x transcription factors. It is well known that MAPK pathways transmit extracellular signals to the nucleus to regulate different cellular processes (Chuderland&Seger 2005, Adachi et al 2000, Chen et al 1992) (Fig. 4).

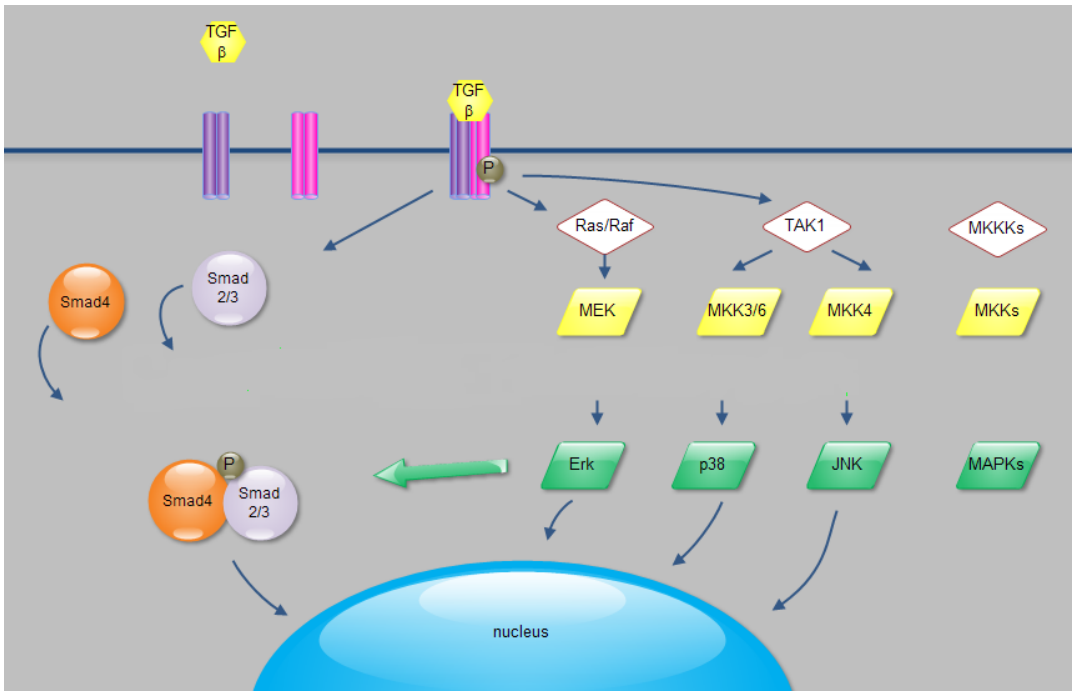

Figure 4. Summary of Smad-dependent and Smad-independent pathways that play role in TGF-β induced epithelial-mesenchymal transition. The formation of TGF-β ligand- receptor

complex activates Smad2/3 proteins that form oligomer complexes with Smad4 and enter the nucleus exerting their effects on target genes. Besides this signaling route, TGF-β ligand-receptor complex activates MAPK pathways (ERK, p38, JNK) that not only carry different extracellular signals towards the nucleus and contribute to the activity of transcription, but MAP kinases also modify the activity of Smad-proteins. The balance between activation of Smad proteins and MAPK pathways defines the cellular responses to TGF-β. For more details, see text. (Source: Balogh et al 2013)

However, it has recently been described that non-Smad signaling proteins (the elements of MAPK cascade) take part in the physiological responses of TGFβ as well by other different mechanisms: i) they can directly modify the activity of Smad proteins by e.x phosphorylation (p38 MAP kinase and JNK kinase have been reported to phosphorylate Smad2/3 and suppress their activity (Kamaraju&Roberts 2005, Mori et al 2004). ii) They can directly interact or be phosphorylated by TβRs, hence a parallel signaling is initiated that might antagonise Smad pathway or iii) non-Smad proteins can directly be modulated by Smads that transmit signals to other pathways (Moustakas&Heldin 2005). Emerging new data reflects the complexity of how the Smad- and non-Smad pathways are interconnected. The ERK MAPK phosphorylates the MH1 domain of Smad2 and blocks its nuclear translocation, thus transcriptional output. TGF-β induced JNK can also phosphorylate Smad3 and induces its translocation to the nucleus (Kretzschmar et al 1999, Engel et al 1999). The role of regulation of TβRs (phosphorylation, ubiquitilation, sumoylation) is also necessary to be elucidated (Kang&Derynck 2009). The phosphorylation of TβRII on tyrosine can contribute to the activation of TGFβ-induced p38 MAPK pathway and also the tyrosine phosphorylation of TβRI is necessary for the initiation of ERK MAPK pathway in response to TGFβ stimulus (Galliher&Schiemann 2007).

Both Smad and MAPK signaling induced by TGF-β work together in a complex cellular network and the subcellular compartmentalization of both Smad and non-Smad proteins might have a role to define signaling activity, thus cellular answers. The signaling elements of MAPK pathways (MAPKKKs, MAPKKs,) are found at the plasma membrane and in the membrane of endosomes, while the activated MAPKs are bound solely to endosomal membranes. Thus, endosomes are crucial cytoplasmic

compartments; as they create a platform and a special environment for the signaling molecules, they can orchestrate the spatial and temporal regulation of different signaling routes (Zehorai 2010, Taub et al 2007).

By now it is accepted that TGFβ induced Smad activation occurs in both lipid rafts/cavolae and non-lipid rafts, but a recent observation suggests that activation of MAPK in lipid rafts/cavolae is specially required for TGFβ induced EMT (Zuo&Chen 2009). The role of raft compartments and endosomes is best characterized in the Raf-MEK-ERK pathway. Raf kinases are localized near the plasma membrane in the cytoplasm through interactions with different anchoring and scaffolding proteins or lipid compounds (Galmiche et al 2008). MEKs are localized in the cytoplasm of resting cells due to their nuclear export signal (NES). They shuttle between the cytoplasm and the nucleus constantly and they serve as cytoplasmic anchors for ERK. With the help of adaptor protein p18, MEKs are localized in the lipid rafts of late endosomes indicating the importance of endosomal compartments. Upon stimulation, ERK dissociates from MEK and through the formation of homodimers ERKs enter the nucleus by active transport mechanism, while as a monomer it can enter the nucleus by passive diffusion. The nuclear export of ERKs is mediated by a MEK dependent active transport mechanism due to their nuclear export signal (Zehorai et al 2010, Taub et al 2007, Adachi et al 2000, Adachi et al 1999, Fukuda et al 1997a, Fukuda et al 1996) (Fig. 5).

DOI:10.14753/SE.2015.1712

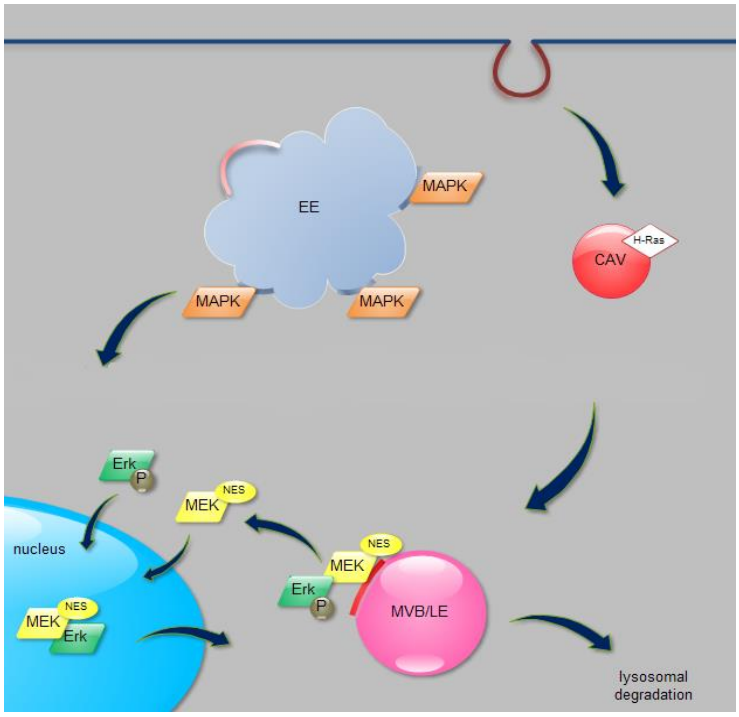

Figure 5. The subcellular localization of ERK MAP kinase pathway. Activated MAPKKK (H-Ras) is localized in lipid rafts/caveolae (CAV). MEK proteins are bound to caveolin-1 positive lipid domains of late endosomal membranes through adaptor proteins and MEKs serve as anchors for ERK. Upon stimulation, ERK dissociates from MEK and enters the nucleus by passive transport and is relocated to the cytoplasm with the help of MEK proteins that has nuclear export signal (NES). For more details, see text. EE: early endosome, CAV: caveola, MVB: multivesicular body, LE: late endosome, P: phosphorylation (Source: Balogh et al 2013)

2.2 The role of ER-α and estradiol in EMT

2.2.1 ER-α as a potential molecular modulator of TGF-β signaling

Recently, estrogen receptor alpha (ER-α) has been suggested as another player in the molecular mechanism of EMT (Guttila et al 2012, Ye et al 2010, Planas-Silva&Waltz 2007). ER-α and TGF-β have opposing roles in cell proliferation and differentiation of epithelial cells. Their regulatory pathways intersect and ER-α blocks the TGF-β pathway at different cellular levels inside the nucleus as well as in the cytoplasm and plasma membrane. Both transcription factors have a prominent role in

maintaining a controlled signaling that is essential for cell and tissue homeostasis and both act in a cell-specific and context-dependent manner (Band&Laiho 2011, Ito et al 2010). For long, estrogen receptors (ER-α, ER-β) have been considered exclusively as transcription factors acting inside the nucleus (Beato et al 1995, Tsai&O'Malley 1994). However, the discovery of its membrane-associated form and the ER–mediated transcription in the absence of its ligand generally changed this concept (Driggers&Segards 2002, Levin 2002). The theory of a hormone-independent ER-α activation that can serve as a mechanism to amplify growth factor pathways (Hall et al 2001) has also been accepted by now.

Besides the nuclear and cytoplasmic pool of ER-α, it has been proved that a small percentage of the receptor (5-10%) resides in the cell membrane and can elicit both genomic and non-genomic responses by activating multiple protein kinase cascades that include MAPK, protein kinase C, Src kinase and PI3K (Levin 2009, Song&Santen 2006, Song et al 2005, Simoncini et al 2004, Razandi et al 1999, Migliaccio et al 1996, Pietras&Szego 1977). There are also data that indicate the role of estrogen-receptor (ER) α as a negative regulator of TGF-β pathway by increasing the degradation of nuclear Smad proteins. ERα forms a protein complex with Smad3/4 and ubiquitin ligases in the nucleus and enhances the degradation of the transcription complex by the ubiquitin-proteasome system (Ito et al 2010).

2.2.2 Extragonadal estradiol: renewal of a traditional belief

The natural ligand of ER-α, estrogen is considered an important morphogen. Meanwhile the concept about ER receptors has largely changed, the renewal of the theory about their ligand effects was essential as well. Besides their gonadal synthesis some articles reported extragonadal estradiol (E2) production ex. in adipocytes, osteoblasts (Bruch et al 1992), chondrocytes, vascular endothelial cells (Bayard et al 1995), aortic smooth muscle cells (Murakami et al 1998), brain tissue (Labrie et al 1997). Thus E2 is no longer solely an endocrine factor, but produced in several extragonadal sites it has the potential to exert its biological effects locally acting as a paracrine or intracrine factor (Simpson et al 2000, Labrie et al 1998, Labrie et al 1997).

DOI:10.14753/SE.2015.1712

The final step in physiological synthesis of 17β-estradiol is aromatization of precursor testosterone by cytochrome P450 aromatase. Aromatase enzyme is essential to convert androgens to estrogens and principally, these extragonadal sites are dependent on circulating C_{19} steroids (DHEA, 4A) as well as testosteron for E2 biosynthesis (Fig. 6). Another important feature is that E2 synthesized within these sites is probably active only at a local tissue level, but the high concentrations achieved presumably exert significant biological influence *in loco* (Simpson et al 1999). Besides the sufficient substrate concentrations, aromatase activity is regulated by several factors in adipocytes. Most important, macrophage-derived pro-inflammatory cytokines such as IL-6, IL-11, TNF-α were reported to upregulate the expression of the enzyme (Simpson et al 2000) that is consistent with other results demonstrating increased aromatase activity in inflammation (Morris et al 2011).

One among the possible cellular processes in which extragonadal estradiol may have regulatory role is autophagy. Recently sex steroids have been described as potential players in the induction of this degradative pathway under inflammatory conditions (Yang et al 2013, Barbati et al 2012).

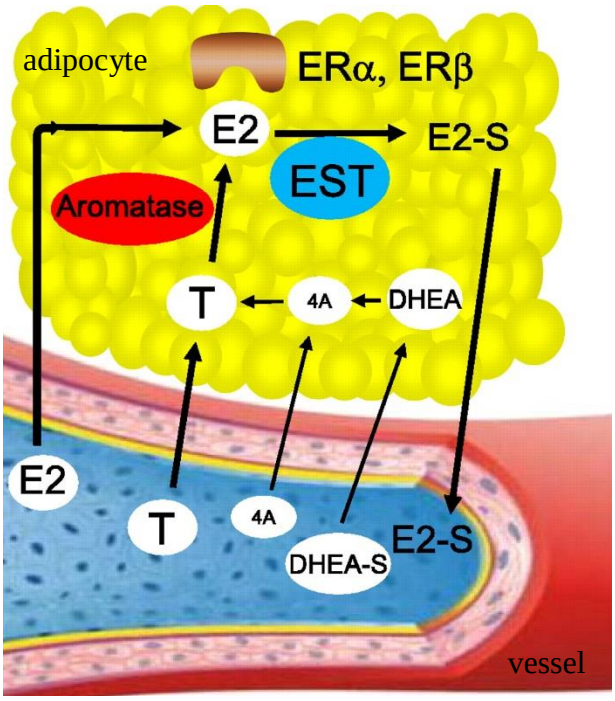

Figure 6. Intracrinology of estrogen in adipose tissue. In premenopausal women, estrogen (E2) functions as a circulating hormone. Conversely, in men and in postmenopausal women, E2 is locally synthesized from androgenic precursors such as testosteron (T), androstendione (4A), or dehydroepiandrosterone (DHEA) in extragonadal sites such as breast, brain, bone, fat. Cellular estrogenic output depends on 1) the ER signaling and sensitivity, 2) the activity of enzymes such as aromatase involved in the biosynthesis of E2 from androgenic precursors, and 3) the inactivation of E2 in E2 sulfate (E2-S), by EST. (Source: Mauvais-Jarvis 2012)

2.3 The role of autophagy in tissue remodelling

Autophagy is a biological process that allows cells to control the number and turnover of intracytoplasmic organelles while maintaining viability upon stress stimuli (Kroemer et al 2010, Levine&Klionsky 2004). The characteristic components of this intracellular degradative pathway are the autophagosomes containing cytoplasmic components targeted into lysosomes for degradation (Levine&Kroemer 2008, Xie&Klionsky 2007). Autophagy is highly conserved across the species, from yeast to mammmals. The identification of autophagy-related Atg proteins and several non-Atg proteins helped to reveal better the regulatory events of the process. Three types of autophagy can be distinguished: besides i) macroautophagy (referred to as 'autophagy' further on) that is best characterized, ii) microautophagy and iii) chaperon-mediated autophagy have been described as well (Mizushima 2007).

The morphological steps of autophagosome formation consists of sequential events including the exfoliation of a double isolating membrane that is further expanding and maturing resulting in a double membrane bound vacuole. The autophagosome fuses with endosomal compartments (MVB/late endosome) creating the so called amphisome. The ultimate fusion of the amphisome with lysosomes results in a single-membrane bound autophago-lysosome in order to degrade the engulfed substances (Mizushima et al 2008, Klionsky 2007, Levine&Klionsky 2004, Ohsumi 2001) (Fig. 7). Several studies have demonstrated that autophagy has a role both in physiological as well as pathophysiological processes (Mizushima 2005). Besides the pivotal role of autophagy in tissue remodelling (Gajewska et al 2013, Mizushima&Komatsu 2011), recent studies demonstrated that autophagy may play essential role in inflammatory processes and

impact the outcome of disease progression (Choi&Ryter 2011, Levine et al 2011). There is a complex reciprocal relationship between the autophagy pathway/proteins and immunity/inflammation; the autophagy proteins function in both the induction and suppression of immune and inflammatory responses, and immune and inflammatory signals function in both the induction and suppression of autophagy (Levine et al 2011).

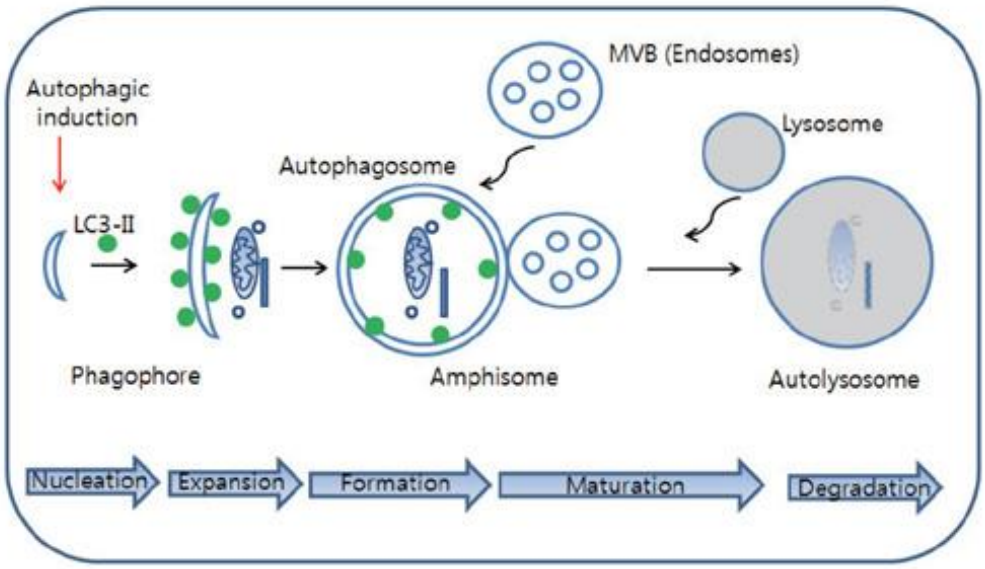

Figure 7. The cellular processes during autophagy. Autophagic process follows distinct stages: nucleation (formation of phagophore), expansion (autophagosome formation), maturation (fusion of autophagosome with MVB (multivesicular body)/lysosome, degradation (acidification). Once autophagy is induced by autophagic stimuli such as inhibition of mTOR, phagophore (isolation membrane) begin to be formed and then cytosolic components are sequestered by autophagosomes characterized by LC3-II-positive double membrane structure. Endosome such as MVB or lysosome can be fused with autophagosome to form amphisome or autolysosome, respectively. In final step, cytosolic components are degraded in autolysosome. (Source: Lee 2012)

DOI:10.14753/SE.2015.1712

3. Objectives

I. Our previous light microscopical results showed that Freund's adjuvant treatment induces remarkable phenotypic changes in mesothelial cells.The first experiments of our studies were directed to certify in detail whether intraperitoneal Freund's adjuvant administration leads to epithelial-mesenchymal transition in mesenteric mesothelial cells *in vivo* by inducing acute inflammation. According to data from literature, TGF-β has an universal role in EMT. We were also interested in revealing whether the cytokine plays role upon inflammation in our system. The following questions were addressed:

1. What are the ultrastructural changes that can be observed in mesothelial cells upon the inflammation and the following regeneration?
2. Can inflammatory cytokines (IL-1, IL-6) be detected in the peritoneal fluid upon Freund's adjuvant treatment?
3. Does TGF-β have any roles in the inflammation-induced epithelial-mesenchymal transition? If so, how the level of its peritoneal secretion correlates with the inflammatory events?
4. Can the elements of the canonical TGF-β signaling pathway be detected in mesothelial cells? If so, what are the cellular compartments along which the signaling molecules (TβRII/Smad7) are accommodated in correlation with the inflammatory events?
5. Does caveolar internalization have a role in the dynamics of TGF-β signaling?

II. Recently, ER-α has been suggested as another player in the molecular mechanism of EMT and has opposing roles with TGF-β in a cell and context-dependent manner. We previously showed that mesothelial cells can assume a macrophage character by expressing ED1 (macrophage marker)

and may serve as a source of peritoneal macrophages upon treatment. Since macrophages are well-known to express estrogen-receptor α (ER-α), we were interested in whether the receptor might be present in mesothelial cells and has a role in TGF-β induced EMT. Based upon our previous results and the data from literature we considered to answer the following questions:

1. Do mesothelial cells express ER-α upon steady state and inflammatory conditions? If so, what is the subcellular distribution of the receptor?
2. Does the level of ER-α expression change during the inflammation?
3. Do ER-α and elements of the TGF-β pathway meet in any cytoplasmic compartments (caveolae, multivesicular bodies)?
4. Is there any natural ligand of ER-α in the peritoneal fluid and if so, how the level of its secretion correlate with the kinetics of inflammation and/or regeneration?

III. The detected and prolonged secretion of extragonadal estradiol raised the question about its possible role in tissue remodelling, regeneration. Among the several factors sex steroids have recently been described to induce autophagy and help in tissue remodelling, thus our interest turned towards examining whether possible estradiol-induced autophagy is present in mesothelial cells following acute inflammation and the process might contribute to the morphological re-establishement of the mesothelium. The following questions were addressed:

1. Is autophagy present and may play role in the removal of cytoplasmic organelles following inflammation? If so, how the rate of autophagy correlates with the inflammatory events and the secreted E2 concentrations?
2. Does extragonadal estradiol have pivotal role in inducing autophagy? Are there any extracellular signals (TNFα) that are present and aid or overwrite the effects of estradiol in our system?

DOI:10.14753/SE.2015.1712

4. Materials and methods

Material and Treatment

Rat mesentery (peritoneum of small intestine) was isolated from control and Freund's adjuvant (Sigma-Aldrich, Steinheim, Germany) treated Sprague-Dawley male rats (200–400 g) (Female rats were used in one experiment, see in Chapter II/1/3). 1 ml complete Freund's adjuvant was injected into the peritoneal cavity. One day (D1), two days (D2), three (D3), five (D5), six (D6) eight (D8) and eleven (D11) days following intraperitoneal injections, prior to sample removal the animals were anaesthetized and sacrificed by decapitation.

Reagents

Primary antibodies used for the morphological experiments were: rabbit polyclonal anti-caveolin-1 antibody (Transduction Laboratories), rabbit polyclonal anti-EEA1 antibody (Abcam), rabbit polyclonal anti-Smad7 antibody (Epitomics). Rabbit polyclonal anti estrogen-receptor alpha antibody (H-184): sc-7207) and rabbit polyclonal TGF-βRII antibody (C-16)-R: sc-220-R were purchased from Santa Cruz. Biotinylated anti-rabbit IgG was used as a secondary antibody at a dilution 1:200 (Vector Laboratories Inc, Burlington, CA). For confocal microscopy, streptavidin Alexa Fluor 488 and 555 conjugates, goat anti-rabbit IgG Alexa Fluor 555 (MolecularProbes, Leiden, the Netherlands) were all used at a dilution 1:200. The nuclei were stained with DAPI (Vector Laboratories Inc, Burlington, CA). For immunogold labeling, protein A conjugated to 10- (1: 50) and 15-nm (1:50) gold particles was manufactured and purchased from Cell Microscopy Centre, Utrecht, The Netherlands.

Besides the above described primary antibodies we further applied in the biochemical experiments anti-TGF-β antibody, polyclonal anti-LC3B antibody purchased from Cell Signaling. Polyclonal anti-pErk1/2 was the generous gift of dr. Márk Oláh and monoclonal anti-tErk1/2 was purchased from Life Technologies. Polyclonal anti-actin antibody and polyclonal anti-rab7 antibody were obtained from Sigma-Aldrich and polyclonal anti-Cd63 antibody was ordered from Santa Cruz. The below inserted table summarizes the sources and applied dilutions of primary antibodies (Table 1).

Table 1. Primary antibodies applied for the experiments.

Antibody	Source	Host	Applied dilutions
anti-caveolin-1	BD, Transduction Laboratories, Lexington, KY	rabbit polyclonal	ICC 1:200 IEM 1:40 IP 1/400 µl
anti-EEA1	Abcam, Cambridge, UK	rabbit polyclonal	ICC 1:200 IEM 1:50
anti-TGFβRII (C-16)-R: sc-220-R	Santa Cruz Biotech Inc. , Santa Cruz, CA	rabbit polyclonal	ICC 1:200 IEM 1:60 IP 2/400 µl
anti-Smad7 (C-terminal)	Epitomics, Burlingame, CA	rabbit polyclonal	ICC 1:20
anti-ER-α (H-184): sc-7207	Santa Cruz Biotech Inc. , Santa Cruz, CA	rabbit polyclonal	ICC 1:200 IEM 1:50 WB 1:300
anti-LC3B	Cell Signaling Technology, Inc., Danvers, MA	rabbit polyclonal	ICC 1:200 WB 1:200
anti-pERK1/2	Cell Signaling Technology, Inc., Danvers, MA	rabbit polyclonal	WB 1:200
anti-tERK1/2	Life Technologies	mouse monoclonal	WB 1:200
anti-actin	Sigma-Aldrich, Co., St. Louis, MO	rabbit polyclonal	WB 1:5000
anti-rab7	Sigma-Aldrich, Co., St. Louis, MO	rabbit polyclonal	WB 1:1000
anti-CD63 (H-193): sc-15363	Santa Cruz Biotech Inc. , Santa Cruz, CA	rabbit polyclonal	WB 1:500
anti-TGF-β	Cell Signaling Technology, Inc., Danvers, MA	rabbit polyclonal	WB 1:1000

Tissue fixation for light and electron microscopy

Mesentery was isolated from both control and Freund's adjuvant-treated animals. The samples were fixed either in a 1:1 mixture of 2 % glutaraldehyde (GA in 0.2 M cacodylate buffer) and 2 % OsO_4 (Os) in distilled water (30 min, on ice) or freshly prepared 4 % paraformaldehyde (PFA) in 0.1 M PB (2-4 h, room temperature). The samples were washed in cacodylate buffer and PBS, respectively and the adipose tissue

was removed from the mesentery. The GA-Os fixed material was proceeded to electron microscopic embedding, while the PFA-fixed samples were used for immunocytochemistry.

Conventional Electron Microscopy

The GA-Os fixed samples were washed in 0.1 M cacodylate buffer three times, dehydrated with ethanol and stained with 1 % uranyl acetate (in 70 % ethanol for 1h, room temperature) prior to araldite embedding. Ultrathin sections were contrasted with uranyl acetate and lead citrate. The samples were analyzed in a Hitachi H-7600 (Tokyo, Japan) transmission electron microscope.

Preparation of semithin and ultrathin cryosections

The PFA fixed samples were stored in 1 % paraformaldehyde (in 0.1 M PB) at 4 °C until further processing. For semithin cryosectioning and immunolabeling, the fixed samples were washed twice in phosphate-buffered saline (PBS), once in 0.02 M glycine/PBS and infiltrated gradually with gelatine solutions of increasing concentrations (2 %, 5 %, 12 % in PB) at 37 °C for 30 min each. The samples were oriented in liquid gelatine and cut into small blocks. For cryoprotection, the blocks were infiltrated with 2.3 M sucrose at 4 °C overnight and afterwards mounted on metal pins, frozen and stored in liquid nitrogen. For preparing semithin and ultrathin cryosections we used Leica Ultracut S ultramicrotome equipped with cryo-attachment (Vienna, Austria). The pickup solution was a 1:1 mixture of 2.3 M sucrose and 1.8 % methylcellulose.

Immunolabeling for light and electron microscopy

0.5 μm semithin sections mounted on microscopic slides were incubated with 0.02 M glycine in PBS for 15 min and they were blocked in PBS containing 1% BSA. Primary antibodies were applied in 1% BSA containing buffer in a humidified chamber at 4 °C (overnight). Prior to a 1 h incubation with the secondary antibodies in a humidified chamber at room temperature, the samples were washed three times with PBS. Sections were then rinsed again with PBS, stained with DAPI, placed under coverslips and

visualized in a Bio-Rad (Ontario, Canada) Radiance 2100 Rainbow confocal microscope.

For cryosectioning and immuno-EM, the fixed tissues were further processed as described (Slot&Geuze 2007). In brief, ultrathin cryosections prepared at −110 °C were transferred to copper grids by pickup with a 1:1 mixture of 2.3 M sucrose in PBS and 1.8% methylcellulose. For immunogold labeling, the grids were incubated first on 2% gelatine/PBS at 37 °C, blocked with 0.02 M glycine/PBS and subsequently incubated with primary antibodies followed by protein A-gold. The sections were contrast stained with 2% uranyl acetate/oxalate, pH 7, followed by 0.4% uranyl acetate pH 4 and 1.8% methylcellulose and dried. The cryosections were analyzed in a Hitachi H-7600 (Tokyo, Japan) transmission electron microscope at 80 kV.

Morphometry and statistical analysis

Twelve to fifteen electron micrographs were taken from three-three parallel biological samples per group. The surface/volume ratio was calculated according to the method described by Weibel et al (Weibel et al 1996). Results were expressed in number of autophage vacuoles per surface area of cell. Statistical analysis was calculated by ANOVA method and Tukey's HSD test using Statistica 11 software (StatSoft Inc., Tulsa, OK).

Isolation of mesenteric mesothelial cells

Prior to removal the mesentery, we first washed the abdominal cavity with 2 ml PBS and then rinsed the removed mesentery in clean buffer for 10 minutes. Subsequently, it was placed into 0.2 % collagenase (in DMEM, Sigma-Aldrich Corp., St Louis, MO). The solid remnants (adipose tissue, connective tissue) were then removed and the samples were washed three times in PBS by centrifugations at 1000 rpm, for 10 min at room temperature. The pellets were then placed into liquid nitrogen for 10 minutes and further stored at -80 °C until use. (qRT-PCR results confirmed the mesothelial phenotype of the retrieved cell population.)

Collection of peritoneal fluid and trunk blood, Chemiluminescence immunoassay

To determine the secretion level of 17β-estradiol in the peritoneal fluid (PF), six to eight samples per group were collected from male animals by washing the peritoneal cavity with 2 ml PBS. The PF samples were centrifuged at 1000 rpm, for 10 min at 4 °C and the supernatants were stored at -20 °C until use for analysis. To determine the estradiol (E2) concentrations in the plasma, we collected the trunk blood of the animals following decapitation. The collected blood was centrifuged at 1500 rpm, for 20 min at 4°C. The gained serum samples were stored until use in a NaCl (0.9%) and EDTA (5%) containing solution at -20 °C. Elecsys Estradiol II assay on Cobas E411 (Basel, Switzerland) was used to measure and determine the plasma and peritoneal hormone concentrations. The significance was tested by the ANOVA method and Tukey's HSD test using Statistica 11 software (StatSoft Inc., Tulsa, OK).

RNA isolation and quantitative RT-PCR

Total RNA was extracted from isolated mesothelial cells with RNeasy tissue mini kit (QIAGEN Inc., Chatsworth, CA). For qualitative and quantitative analysis of RNA preparations, RNA 6000 Nano Chip kits in an Agilent 2100 Bioanalyzer (Agilent Technologies Inc., Santa Clara, CA) was used according to the manufacturer's instructions. Following RNA isolation, RNAs obtained were transcribed into cDNAs using SuperScript™ III First-Strand Synthesis SuperMix (Life Technologies, Carlsbad, CA), according to the manufacturer's instructions. From each samples, 0.5-1 μg of total RNA was converted into cDNA. Real-time PCR was performed using Taqman Universal Master Mix II, No UNG and the 7900HT Real-Time PCR System (Life Technologies, Carlsbad, CA), with the following parameters: 50 °C for 2 min and 95 °C for 10 min, followed by 40 two-step cycles at 95 °C and at 60 °C for 1 min. Applied Biosystems pre-designed TaqMan® Gene Expression Assays were used for real-time PCR (Il6 Rn00561420_m1, Il1a Rn00566700_m1, Il1b Rn00580432_m1, Esr1 Rn00664737_m1, Tnf. Rn00562055_m1, GAPD.4352338E and B2m Rn00560865_m1). The qRT-PCRs were executed in triplicate using TaqMan probe synthesized by Applied Biosystems). SDS 2.3 (Applied Biosystems, Foster City, CA) and RQ manager 1.2 softwares (Applied Biosystems, Foster City, CA) were applied for calculation of the threshold cycle (Ct) values in each sample.

Expression level was calculated by the ddCt method, and fold changes (FC) were obtained using the formula 2^{-ddCt}. Computed internal control corresponding to the geometric mean of Ct values of the two housekeeping genes (GAPD and B2m) was used for the ddCt calculation. Gene expression levels at different time points were compared to controls using ANOVA and t-test with a statistical software SPSS version 19 (SPSS Inc., Chicago, IL, USA).

Immunoprecipitation

Immunoprecipitation was performed by standard methodologies. Briefly, isolated mesothelial cells from D3-D5 samples were lysed in 1 ml solubilization buffer (50 mM Tris-HCl, pH 7.5, 150 mM NaCl, 1 mM EDTA, 1 mM Na_3VO_4, 1 mM NaF, 10 % glycerol, 0.5 % Nonidet P40, 0.1 mM PMSF, 10 µg/ml aprotinin. The lysates were then incubated with specific antibodies, anti-caveolin-1 and anti-TGF-βRII for 5 h at 4°C. Immune complexes were formed by addition of protein-A-Sepharose 4B (Sigma) and incubated for 1 h at 4°C. The immune complexes were then sedimented by centrifugation at 12,000 G, followed by 4-5 washes in lysis buffer. Bound proteins were solubilized and analyzed on SDS-PAGE, followed by immunoblotting.

Western blotting

The pellets of isolated mesothelial cells were dissolved in 1ml lysis buffer containing 50 mM Tris-HCl pH 7.5, 150 mM NaCl, 2 mM EDTA, 200 mM Na_3VO_4, 1 mM NaF, 1 % Nonidet P-40 and protease inhibitor mixture (Complete, Mini, Roche). Insoluble material was removed by centrifugation with 1000 rpm for 10 min. The protein contents were determined by the Bradford method (Bradford 1976) and diluted to a concentration of 0.5 mg/ml. Afterwards the samples were mixed with the same amount of reducing Tris-SDS buffer (Tris 0.5 M pH 6.8, 10 % glycerol, 2% SDS, 0.00125 % bromophenol blue, 0.5 % mercapto-ethanol) and heated at 95 °C for 4 min. 20 µl per well from the samples were loaded onto an Acrylamide/Bis gel and separated by electrophoresis. After separation, proteins were transferred onto a nitrocellulose membrane (Amersham, GE Healthcare Biosciences, Pittsburgh) in a buffer containing Tris–Glycine pH 8.3, 0.1 % SDS and 20 % methanol. Aspecific reactions were blocked by placing the membrane

at room temperature for 2 h in PBS-Tween (0.5 M PBS, Tween 0.05 %) containing 5 % skim milk powder. The membranes were then incubated with primary antibodies diluted in PBS-Tween containing 0.5 % bovine serum albumine at 4 °C for overnight. After washing in PBS-Tween the membranes were treated with species-specific peroxydase-conjugated secondary antibodies (Amersham, GE Healthcare Biosciences, Pittsburgh) for 1 h at room temperature. The labeled protein bands were visualized by the ECL Plus chemiluminenscence method and developed onto high performance chemiluminescence film (Amersham, GE Healthcare Biosciences, Pittsburgh). Relative optical densities were measured using the ImageJ software (U. S. National Institutes of Health, Bethesda, Maryland) and the results of three to four independent experiments were compared and statistically analyzed. The significance was tested by the ANOVA method and Tukey's HSD test using Statistica 11 software (StatSoft Inc., Tulsa, OK).

DOI:10.14753/SE.2015.1712

5. Results

5.1 The morphological characterization of TGF-β induced EMT in mesothelial cells *in vivo*

5.1.1 Ultrastructural evidences of type II EMT

In untreated, control animals mesothelial cells form a continuous simple squamous epithelial layer on both sides of the mesentery. As observed in the electron microscope, the cytoplasm of these cells was rather poor in cell organelles and the cells were dominated by the nucleus. A continuous basal membrane separated the mesothelial cells from the underlying connective tissue and maintained the integrity of the mesothelial layer. Caveolae (caveolin-containing lipid rafts seen as flask-shape invaginations of the cell membrane) were abundantly present on the basolateral and apical surfaces of the cells (Fig. 8 A).

Our previous light microscopical data revealed that mesothelial cells lose their epithelial character (decreased cytokeratin and E-cadherin expression) upon Freund's adjuvant treatment and assume a mesenchymal phenotype by expressing vimentin (Katz et al. 2012). Upon inflammatory stimuli (Freund's adjuvant treatment) remarkable changes appeared in the ultrastructure of mesothelial cells as well. The dynamics of these changes showed a culmination on the second to third day (D2/D3) after treatment. From the fifth day (D5) on the tissue started to recover and the repairment was morphologically accomplished by the eleventh day (D11).

Characteristic ultrastructural changes were the disintegration of basal membrane and transformation of the squamous mesothelial cells into individual cuboidal-shaped cells in two days after treatment (Fig. 8 B). By the fifth day, the cells developed numerous lamellar processes and became spindle-shaped (Fig. 8 C). The cytoplasmic compartments were more prominent: an increased number of mitochondria, polyribosomes, numerous vesicles and a growing number of multivesicular bodies (MVBs) could be observed in parallel with the inflammatory events of the surrounding tissue from D3. A striking observation was the presence of thickened, electron-dense

DOI:10.14753/SE.2015.1712

domains on the limiting membrane of MVBs with a fine coat of medium electron density on the cytosolic side (Fig. 8 D). These specific membrane domains (referred from now on as MVB plaques) disappeared by the later stages of the MVB maturation process (by D5) and could not be observed in the membrane of intermediate forms between MVB and lysosome (Fig. 8 E). By D11 mesothelial cells retrieved their flat morphology and became integrated with the underlying connective tissue by the rearrangement of the basal lamina (Fig. 9 A). Furthermore, the neighbouring mesothelial cells came into contact with each other via reassembling intercellular adhesions (tight juctions, adherens junction) thus completing an uniform mesothelial layer again (Fig. 9 B).

DOI:10.14753/SE.2015.1712

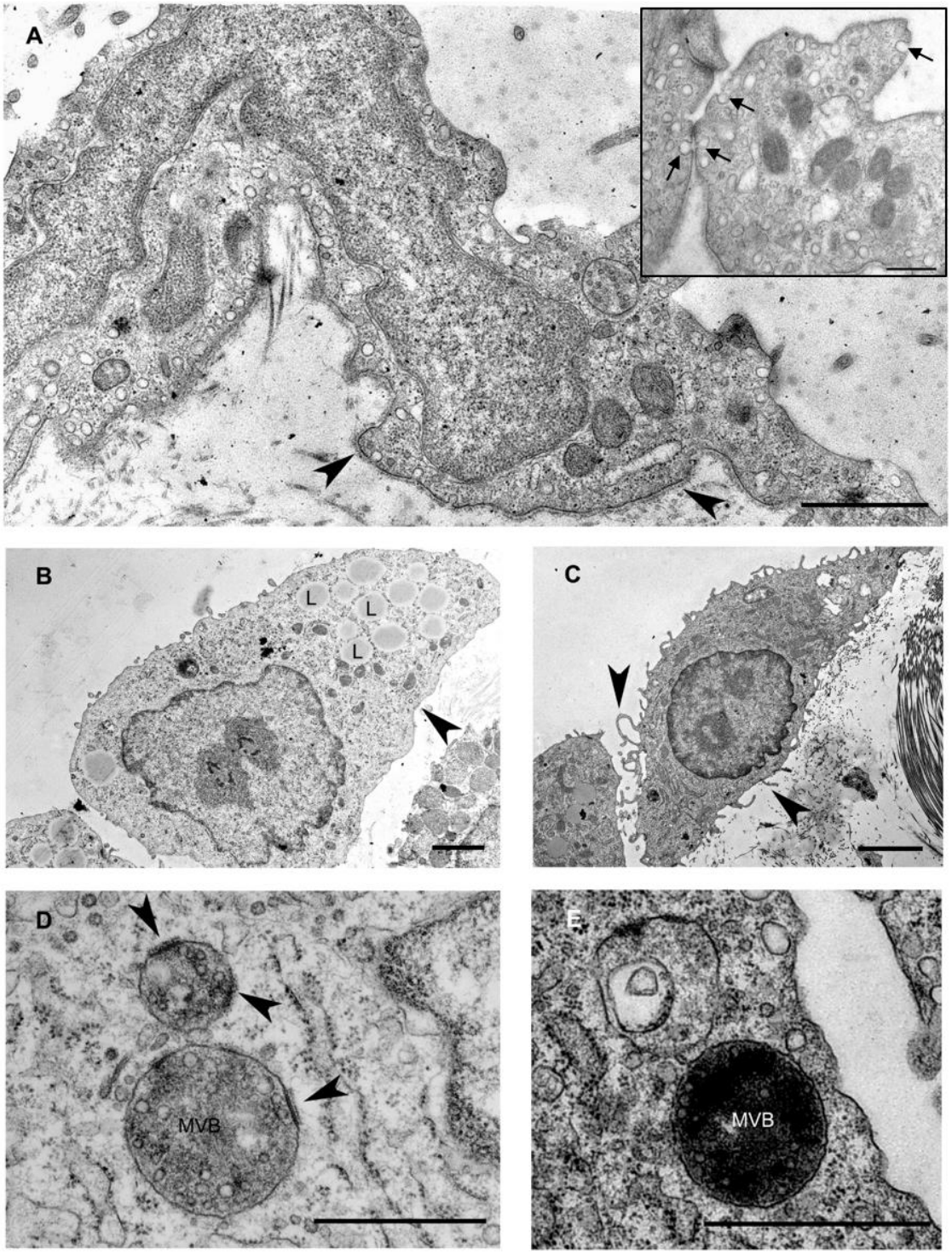

Figure 8. Fine structural aspects of EMT in mesothelial cells upon Freund's adjuvant treatment A Non-treated (control) cells are flat and form a continuous layer on the basal lamina (arrowheads). Caveolae are abundantly present in the control cells seen as small flask shape invaginations of the plasma membrane (insert box, arrows). **B** Upon inflammation, at D2 mesothelial cells progressively lose the connection with the underlying connective tissue as the

basal lamina becomes discontinuous and disintegrates (arrowhead). The cytoplasm of mesothelial cells contains lipid droplets (L) that are probably identical with internalized Freund's adjuvant oil droplets. **C** On the fifth day of treatment, mesothelial cells assume a spindle-shape morphology with several villar or lamellar processes (arrowheads) on their surface. **D** An increasing number of multivesicular bodies (MVB) appear from D3. Note specific membrane domains of the organelles (arrowheads) showing an increased density and apposition of a coat on the cytosolic side (MVB plaques). **E** The MVB plaques disappear by the later stages of MVB maturation, by D5. Scale bars: (A) 1μm, insert 400nm (B) 2μm (C) 2.9μm (D) 500 nm, (E) 1μm.

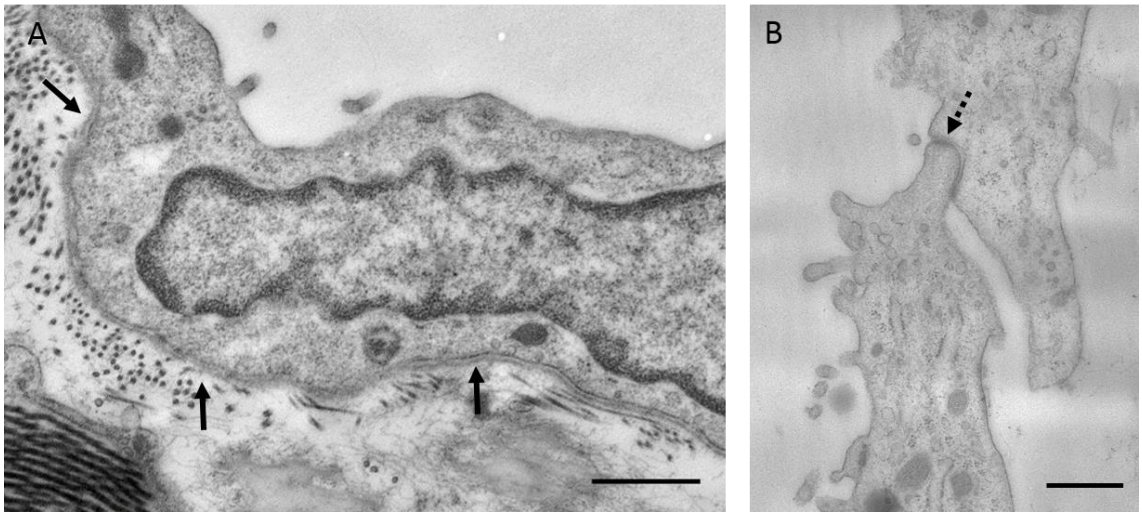

Figure 9. Electron micrographs showing mesothelial cells eleven days after Freund's adjuvant treatment. A Note the continuous basal lamina (arrows) and the flat morphology of mesothelial cell. **B** Reassembly of intercellular junctions (tight or adherens junctions) (dashed arrow) could be observed between the neighbouring mesothelial cells at this time. Bars indicate 833nm

DOI:10.14753/SE.2015.1712

5.1.2 Inflammatory cytokines and TGF-β are released into the peritoneal cavity upon Freund's adjuvant treatment *in vivo*

In addition to the observed ultrastructural changes, it was of primary importance to see if Freund's adjuvant treatment induces inflammatory responses in our *in vivo* system at a molecular level as well. To verify this, we determined the expression levels of pro-inflammatory cytokines in mesothelial cells as they are well-known to be involved in immune responses and inflammatory processes. The results of quantitative RT-PCR showed that mRNA expression levels of interleukin type 1alpha and type 1beta and also interleukin 6 increased in mesothelial cells in response to Freund's adjuvant treatment (Fig. 10 A). The elevated mRNA levels of these cytokines correlated with the dynamics of the observed morphological changes during the inflammatory events: expression levels of mRNAs had a peak on D3 followed by a significant downregulation that could be observed from the fifth day indicating the termination of the inflammatory response.

TGF-β has an universal role in EMT. While the observed morphological changes seemed identical with the steps of EMT, it was pivotal to see whether TGF-β plays role in our system as well. The Western blot data proved that TGF-β was secreted into the peritoneal cavity upon inflammation and showed a peak between D2 and D3 (Fig. 10 B-C). The alterations in the secretion of the cytokine were in accordance with the observed morphological changes as well as with the expression levels of inflammatory cytokines indicating its role in EMT.

DOI:10.14753/SE.2015.1712

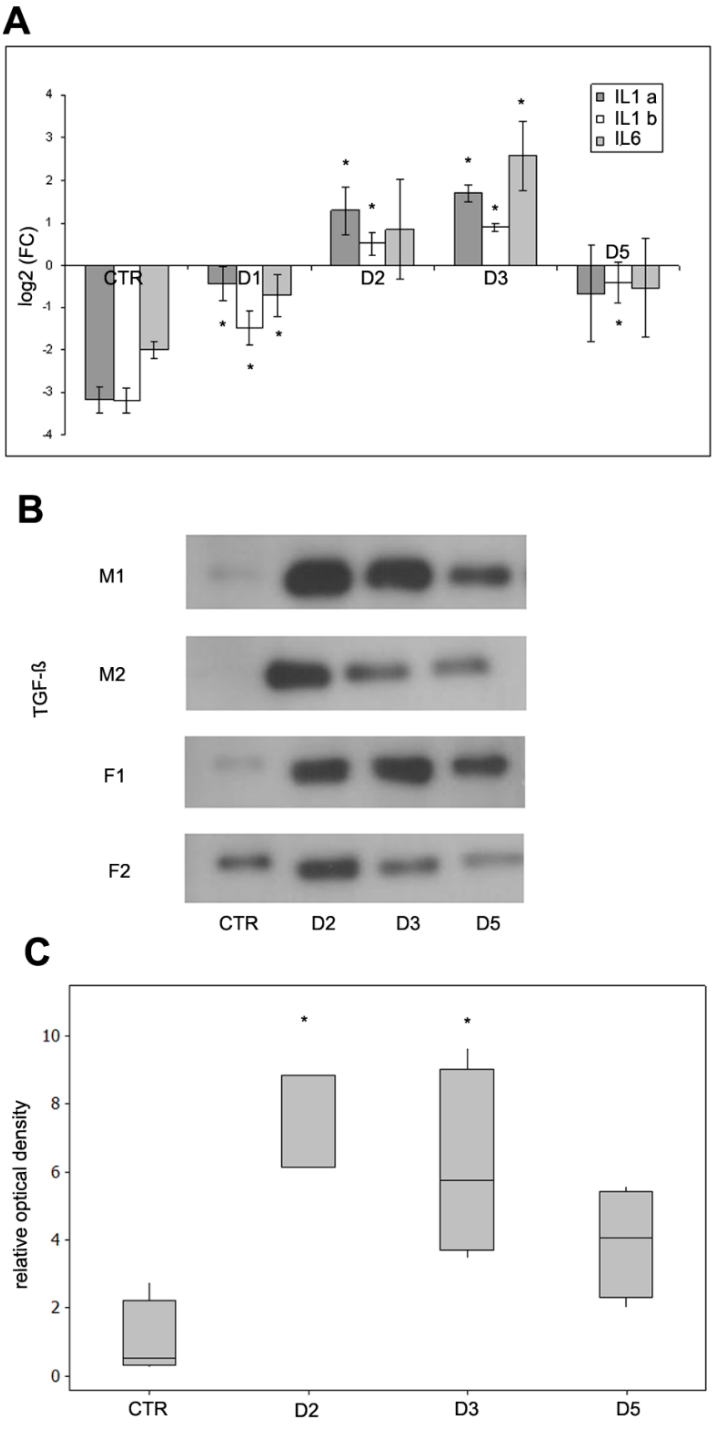

Figure 10. Expression levels of proinflammatory cytokines in mesothelial cells and peritoneal secretion of TGF-β in response to Freund's adjuvant treatment. A The mRNA expression levels of IL-1alpha (IL1a), IL-1beta (IL1b) and IL-6 increase significantly until the third day where expression levels reach a maximum. Further on a decline was observed and reached a similar level measured at the beginning of inflammation induction. **B** The secretion of

TGF-β (measured by Western blot using Pan-TGF-β antibody, 46kDa) in the peritoneal cavity follows the same pattern. **C** The relative levels of secreted TGF-β were measured by densitometry. The asterisks show significant differences from the control group ($p < 0,05$).
M: male F: female

5.1.3 The morphological detection and the subcellular distribution of the main canonical TGF- β signaling molecules in mesothelial cells

To map whether the elements of TGF-β signaling are present in mesothelial cells, we selected major downstream molecules (TβRII&Smad7) that are considered indispensable either in the promotion or in the termination of the signaling.
Upon ligand binding, TGF-βRII is responsible for the transmission and promotion of the signaling. We determined the subcellular localization of the receptor by using immunocytochemical approach: our confocal microscopical results showed that the receptor was located both along the plasma membrane as well as inside the cytoplasm. Under steady state conditions, intracellular receptor labeling appeared in early endosome antigen-1 (EEA1) positive compartments (Fig. 11 A-C). By D3 the majority of the detected TβRII labeling occured inside the cytoplasm (Fig. 11 D-F) and was predominantly found in vesicular (punctate) structures overlapping substantially with EEA1. By D5 numerous large colocalization puncta could still be identified in the cytoplasm of mesothelial cells (Fig. 11 G-I).

DOI:10.14753/SE.2015.1712

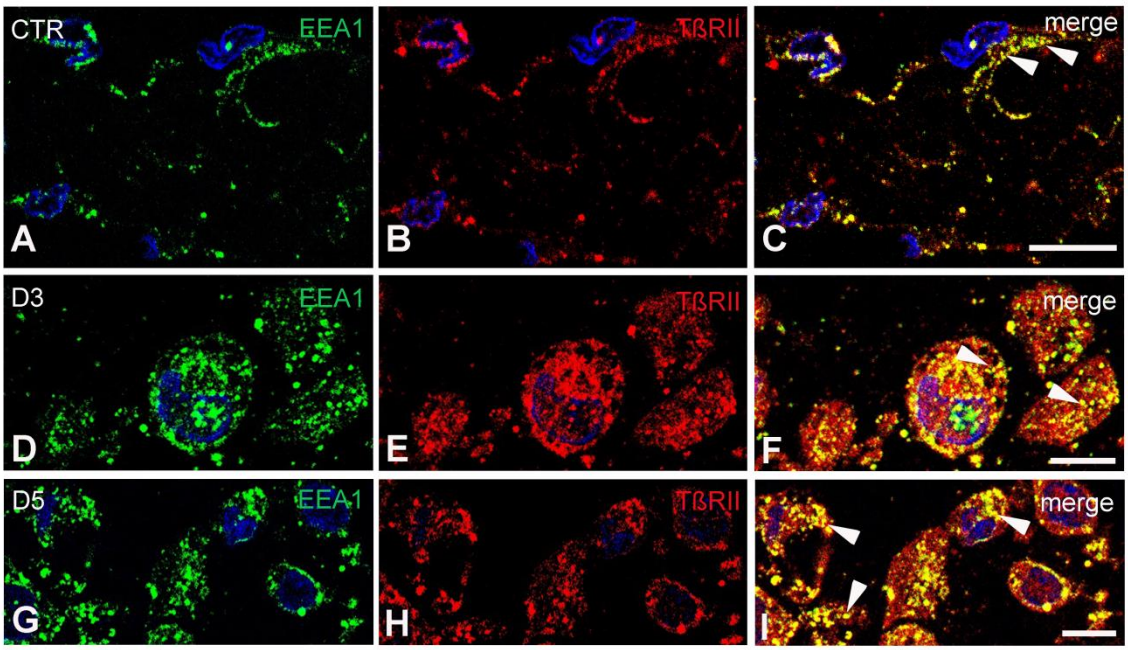

Figure 11. TGF-βRII is abundantly present and mainly accommodated in early endosome antigen-1 positive compartments in control and treated mesothelial cells. Semithin frozen sections labeled with antibodies directed against TβRII (red) and early endosome antigen-1 (EEA1) (green). **A-C** In control mesothelial cells, TβRII could be detected either along the plasma membrane or in EEA1 positive early endosomes (arrowheads). **D-F** By D3, the receptor labeling entirely fulfilled the cytoplasm where it was found in vesicular structures overlapping substantially with EEA1 (arrowheads). **G-I** By D5, colocalization of TGFβRII and EEA1 was still pronounced in the cytoplasm of mesothelial cells (arrowheads). Nuclei were stained with DAPI, bars indicate 10μm.

Since caveola-mediated internalization of TβRs presumably enhance the termination of TGF-β signaling, it was of great interest to see whether the receptor shows colocalization with caveolin-1 positive lipid domains and/or caveolae at any time of the inflammation in mesothelial cells *in vivo*.

We carried out double immunolabeling on semithin frozen sections and we found that in control mesothelial cells TβRII could not be detected together with caveolin-1 (Fig. 12 A-C). At the peak time of inflammation (D3), however TβRII abundantly appeared all

over the cytoplasm of mesothelial cells and several overlapping puncta (indicating colocalization) could be observed between the two markers (Fig. 12 D-F). With the progression of inflammation, by D5 substantial cytosolic co-labeling between TβRII and caveolin-1 was present in mesothelial cells (Fig. 12 G-I).

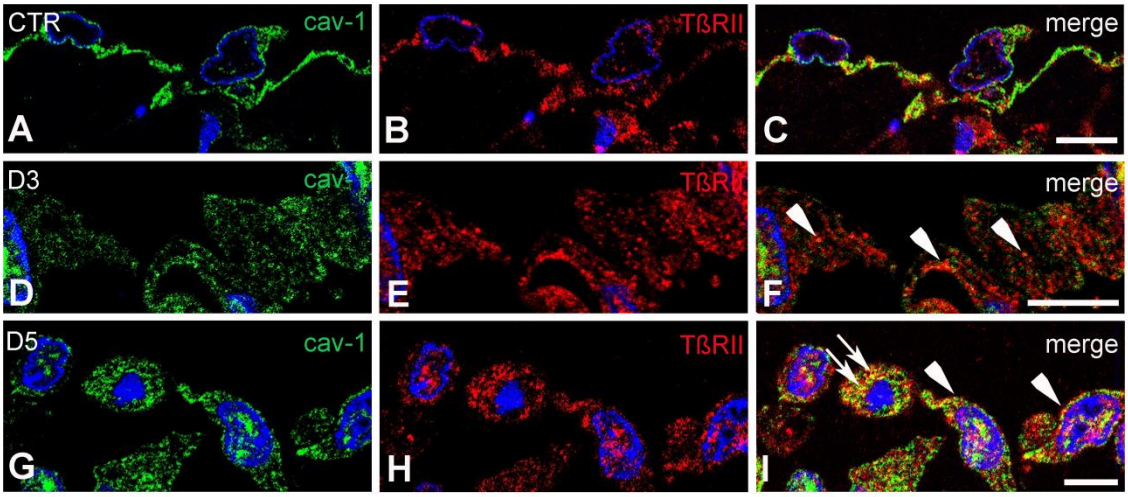

Figure 12. The occurence of TβRII in caveolin positive lipid domains/caveolae upon inflammation. Semithin frozen sections immunolabeled with antibodies directed against TβRII (red) and caveolin-1 (green). **A-C** In untreated mesothelial cells, TβRII appeared separately from caveolin-1 labeling. **D-F** By the peak time of inflammation (D3), the receptor labeling was found all over the cytoplasm overlapping with caveolin-1 (arrowheads). **G-I** By D5, several orange (colocalization) puncta could be identified at the periphery (arrowheads) as well as in the cytoplasm (arrows) of the cells. Nuclei were stained with DAPI, bars indicate 10μm.

Among the inhibitory Smad proteins, Smad7 has a pivotal role in the termination of TGF-β signaling. Since there were data showing that the active TβR complex binding Smad7 is targeted and located in caveolin containing lipid domains of the plasma membrane, we also tried to approve this in our system. To obtain data about the presence and localization of the protein we carried out double immunolabeling on semithin frozen sections. Smad7 protein was barely detectable morphologically in mesothelial cells. However on D3 samples the protein was expressed and could be observed both inside the cytoplasm as well as along the plasma membrane. Whenever

DOI:10.14753/SE.2015.1712

we could detect Smad7 at the plasma membrane, it showed colocalization with caveolin-1 (Fig. 13 A-C)

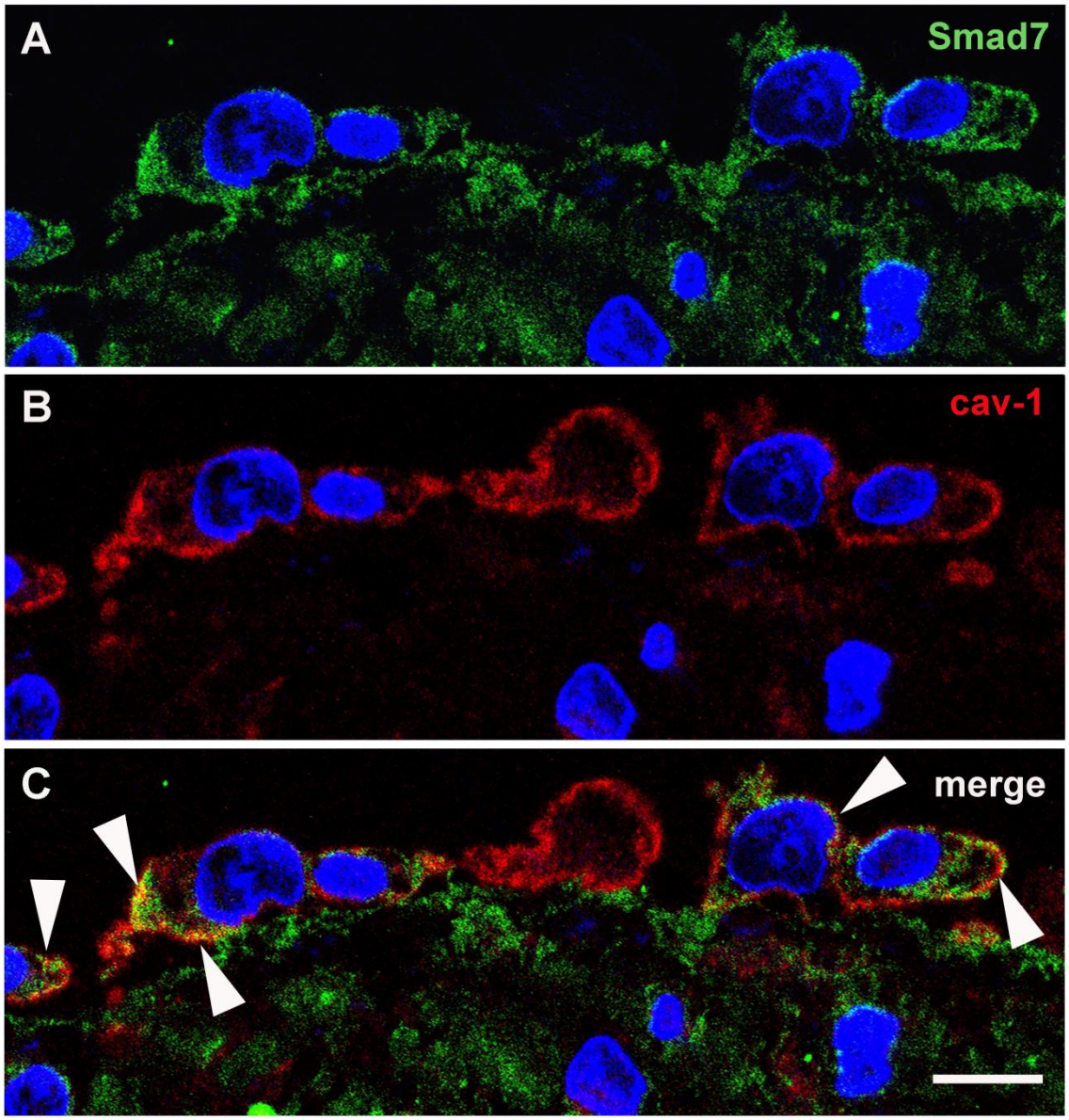

Figure 13. Subcellular distribution of Smad7. **A-C** Immunofluorescence labeling with antibodies directed against Smad7 (green) and caveolin-1 (red). Smad7 labeling could be detected in mesothelial cells from D3 when it appeared both inside the cytoplasm and along the plasma membrane. The plasma membrane protein labeling showed colocalizaton (orange) with caveolin-1 (arrowheads). Bar indicates: 10µm.

DOI:10.14753/SE.2015.1712

5.1.4 En route to multivesicular bodies: the possible role of caveolar internalization in TGF-β signaling pathway

During inflammation related EMT, a notable increase in the number of cell organelles could be observed in mesothelial cells. As MVB formation is a crucial compartment of the classical endocytic pathway for degrading internalized cargos, we investigated whether MVB formation was facilitated concomitant with the inflammatory events. However, we could detect MVBs even under control conditions (Fig. 7 A), their number has remarkably increased by D2 (Fig. 14 B). This increase culminated the following day when numerous mature multivesicular endosomes fulfilled the cytoplasm of mesothelial cells (Fig. 14 C). (MVBs were identified in each case by the presence of the characteristic intraluminal vesicles). As inflammation eased, by D5 the inner content of these endosomes became more homogenous and were identified as lysosomes (Fig. 14 D). Morphometric analysis also confirmed that there was a remarkable increase of forming/mature MVBs two to three days after Freund's adjuvant treatment in mesothelial cells (Fig. 14 E).

The high number of MVBs also indicated that degradative events, thus attenuation of TGF-β signaling has already been started at D3. Therefore, we investigated whether TβRII might appear in endosomal compartments downstream of early endosomes. Our immunoprecipitation results showed that three days after treatment, TβRII was co-immunoprecipitated with multivesicular body marker, Cd63. In contrast, this could not have been observed by D5 when TβRII was already not associated to Cd63 (Fig. 14 F).

DOI:10.14753/SE.2015.1712

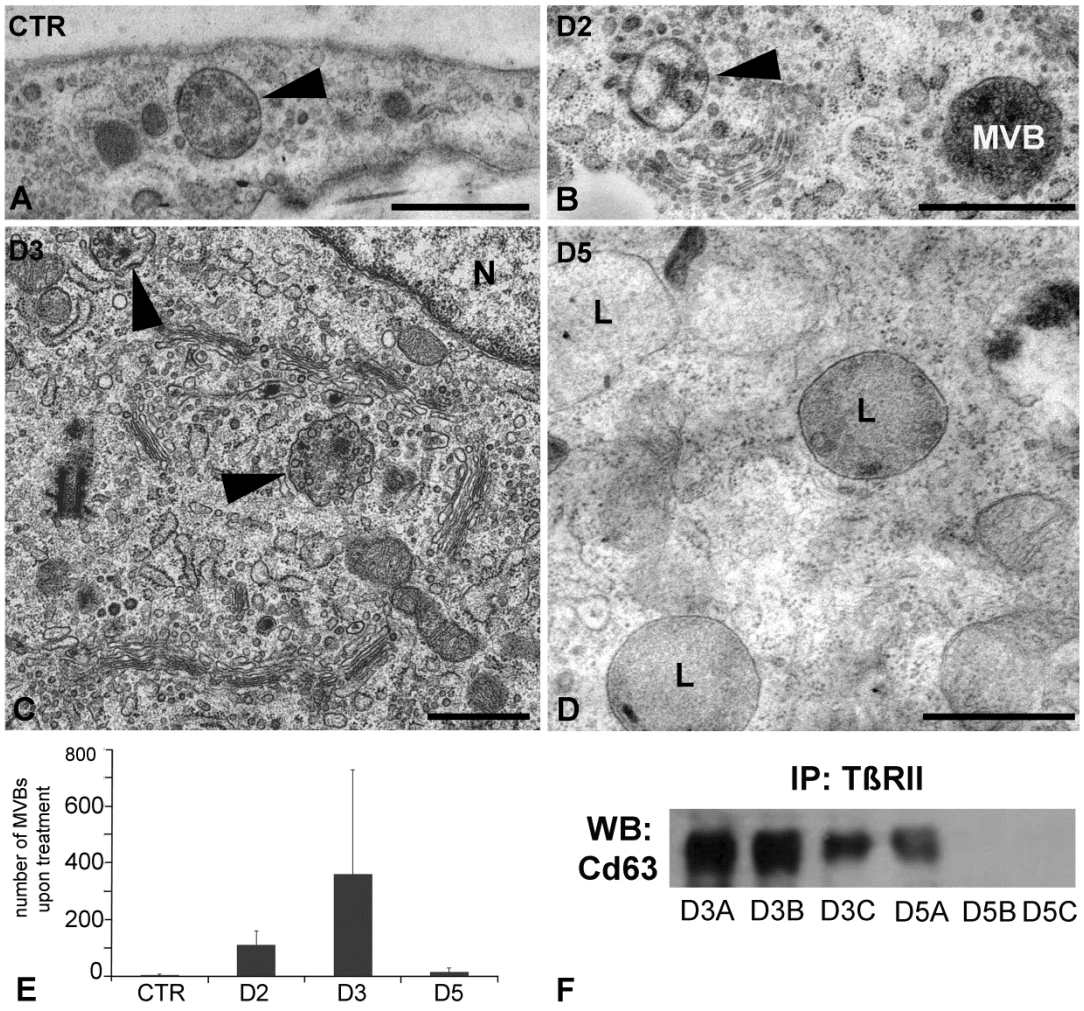

Figure 14. Multivesicular body formation (MVB) and TGFβRII degradation. A Our electron micrographs showed that MVB containing intraluminal vesicules (arrowhead) are present even in control mesothelial cells **B** By D2, several forming (arrowhead) or mature MVBs could be found in the cytoplasm of the cells. **C** Three days after treatment, MVBs were abundantly present around the Golgi-apparatus or at the periphery of the cells **D** By D5, several lysosome-like structures (L) with homogenous density fulfilled the cytoplasm of mesothelial cells. Bars indicate: 1 µm. **E** Our morphometric data further confirmed that MVB formation was indeed facilitated two to three days after treatment (Morphometric analysis was assessed as described by Weibel et al (Weibel et al 1996)). **F** When TβRII was immunoprecipitated with MVB marker, Cd63 we found a strong association of the two proteins by D3. (One parallel biological sample (D5A) in this experiment showed a delayed reaction time for the treatment).

DOI:10.14753/SE.2015.1712

Since there were several reports demonstrating that after caveola-mediated endocytosis TβRs are degraded in lysosomes, we investigated whether caveolae (thus the internalized cargos as well) meet the endo-lysosomal system.

We carried out early endosome antigen-1 and caveolin-1 double-labelled immunofluorescence assay. As it was predicted, in control mesothelial cells there was no detectable colocalization between the two compartments (Fig. 15 A-C). In contrast, by D3 there were numerous colocalization puncta underneath the plasma membrane of the cells indicating that the two markers, thus the compartments they label meet (Fig. 15 D-F). By D5, colocalization between EEA1 and caveolin-1 could still be observed, however to a much lesser extent (Fig. 15 G-I). To further confirm the observed colocalization, we carried out double immunolabeling on ultrathin frozen sections. In fact, the finer morphological results were consistent with the light microscopical data. By D3, we detected endosomes immunopositive for both EEA1 and caveolin-1 markers and these compartments were corresponded to forming MVBs. Several caveolin-1 labeling and EEA1 labeling could be observed either together or individually but consistently labeling the same limiting membrane of forming MVB (Fig. 16 A-B).

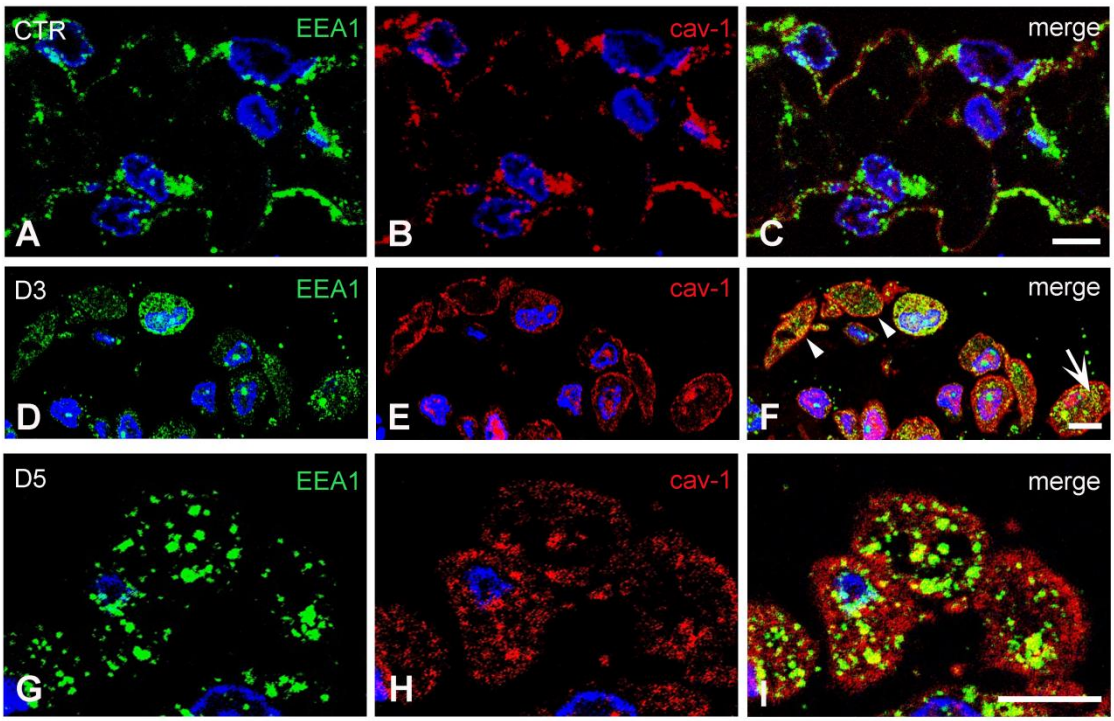

Figure 15. Immunofluorescence detection for possible colocalization between caveolae and early endosomes. Semithin frozen sections labeled with antibodies directed against EEA1

(green) and caveolin-1 (red). **A-C** In control mesothelial cells, no colocalization could be observed between the two markers and labelings appeard separately. **D-F** By D3, however we could detect double labelled structures inside the cytoplasm (arrow) or in the close vicinity of the plasma membrane (arrowheads). **G-I** By D5, colocalization between the two markers could still be observed, however to a much lesser extent. Nuclei were stained with DAPI, bars indicate 10μm.

DOI:10.14753/SE.2015.1712

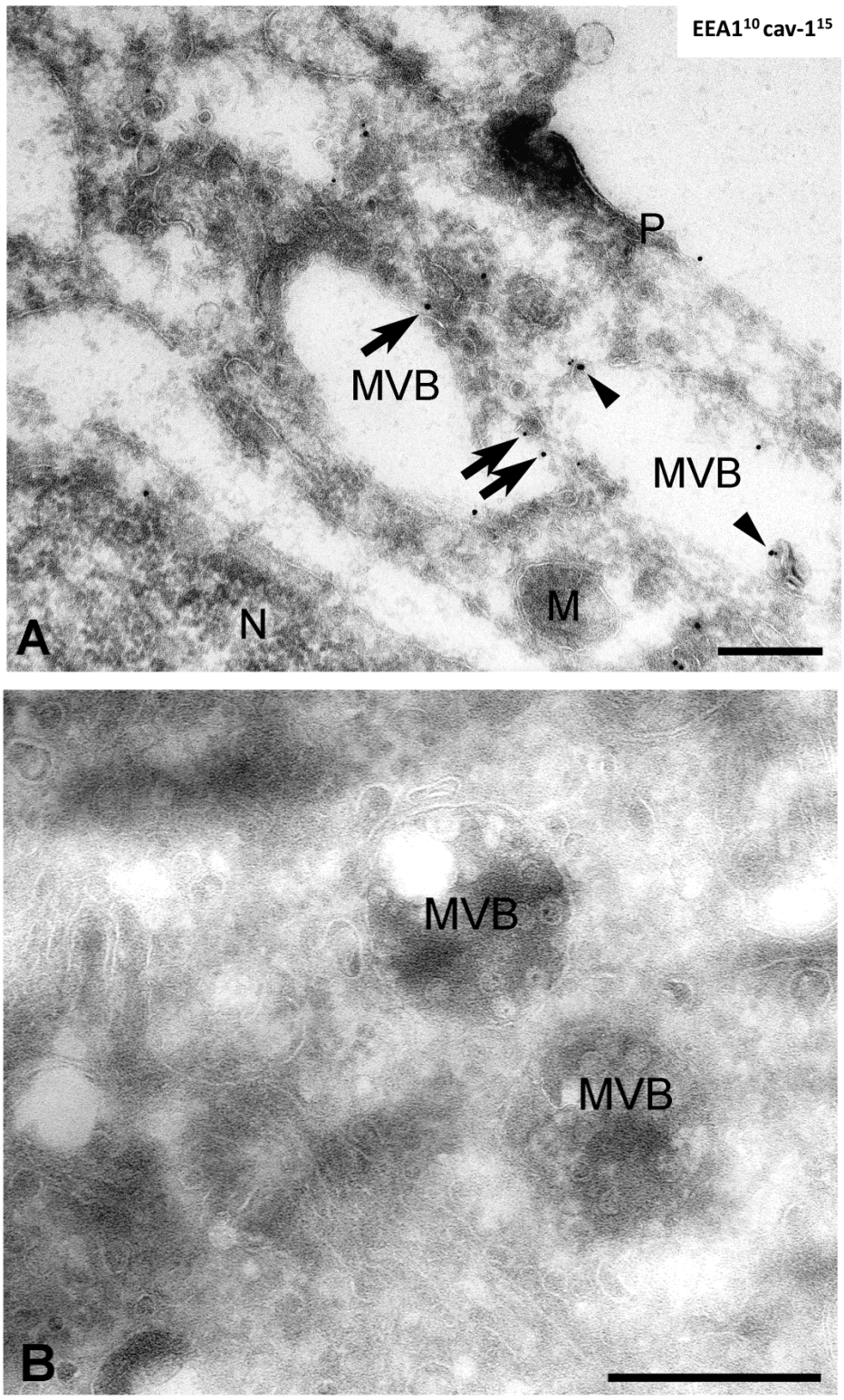

Figure 16. EEA1 and caveolin-1 double-labeling on ultrathin crysections. EEA1 labeled with 10 nm and caveolin-1 with 15 nm gold particles. **A** When multivesicular body (MVB) formation was detected at D3, caveolin-1 and early endosome antigen-1 markers labelled with gold particles were found to be present on its limiting membrane.

Caveolin-1 and EEA1 labelings could be observed either together (arrowheads) or individually (arrows), but consistently on the same endosomal membrane, the mebrane of forming MVB. **B** MVBs on ultrathin cryosections (negative control). M: mitochondrium, N: nucleus Bars indicate: **a** 333 nm**b** 500 nm

Our morphological data was further affirmed by the immunoprecipitation results (Fig. 17 A). On D3 samples caveolin-1 was found to be associated with multivesicular body marker Cd63. In contrast, by D5 caveolin-1 was co-immunoprecipitated with rab7 antibody (marker of late endosomal trafficking downstream of MVBs) (Fig. 17 A). Our Western blot analysis also revealed that caveolin-1 is entirely degraded at a protein level by D6 and only by D11 - with the morphological restitution of mesothelial cells - reached again detectable level (Fig. 17 B).

DOI:10.14753/SE.2015.1712

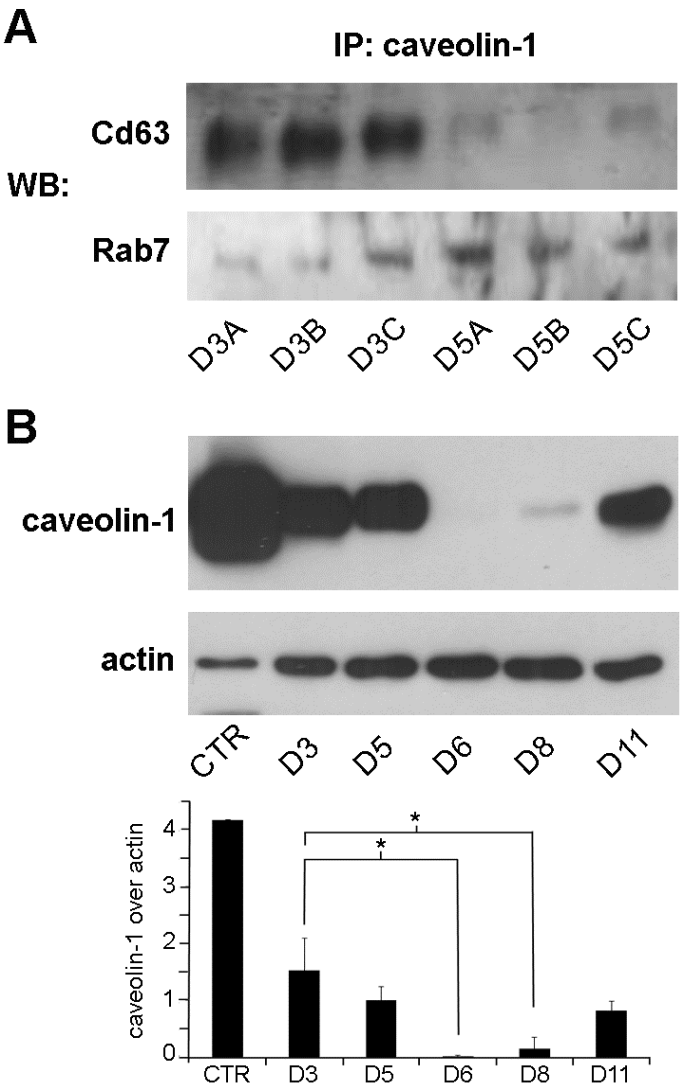

Figure 17. Caveolin-1 is degradaded via the classical endocytic pathway. A At the peak time of inflammation (D3), caveolin-1 was found to be intensively co-immunoprecipitated with Cd63 and later on, by D5 it associated with lysosomal marker, Rab7. **B** Western blot results also affirmed that caveolin-1 (24kDa) expression gradually decreased and could no longer be detected at a protein level by D6. When restitution of mesothelium has been completed, by D11, caveolin-1 expression started to increase. Densitometry analysis showed significant decrease in caveolin-1 expression from D3. Error bars represent standard deviation, asterisks indicate: $p<0,05$.

DOI:10.14753/SE.2015.1712

5.2 The possible role of ER-α and estradiol in EMT

5.2.1 Estrogen receptor alpha (ER-α) expression and its subcellular distribution in mesothelial cells

Data from literature demonstrated the modulator role of ER-α in TGF-β signaling, thus a potential role of the protein in EMT as well. Our previous work proved that mesothelial cells can serve as one of the sources of activated macrophages upon Freund's adjuvant treatment and it is known that macrophages express ER-α. Thus, the question arose whether mesenteric mesothelial cells also express estrogen receptor-α? Our present results show that ER-α is present in mesothelial cells both under steady state and inflammatory conditions. As control cells were flat and the cytoplasm formed a thin rim around the nucleus, it was difficult to define the exact nuclear, cytoplasmic or plasma membrane (PM) localization of the marker with light microscope (Fig. 18 A). The morphological changes of the cells upon inflammation enabled us to better detect the localization of ER-α. Confocal microscopical results after immunofluorescence detection of ER-α showed that labeling appeared in the nucleus, cytoplasm as well as in the plasma membrane and on the consecutive days after treatment the intensity of the labeling increased (Fig. 18 B-D). In those mesothelial cells that had entirely lost the connection with the basal lamina, significant ER-α labeling was found on the plasma membrane and this distribution was clearly apparent on D5 samples (Fig. 18 D). Distribution of labeling along the PM had changed during the inflammatory process: while in control samples the labeling showed a continuous line at the PM (Fig. 18 A), it clustered at certain areas of the plasma membrane in treated cells (Fig. 18 B-D).

Since we found no detectable differences in ER-α labeling between female and male animals, we further carried out our experiments with samples taken from male rats if not indicated otherwise.

DOI:10.14753/SE.2015.1712

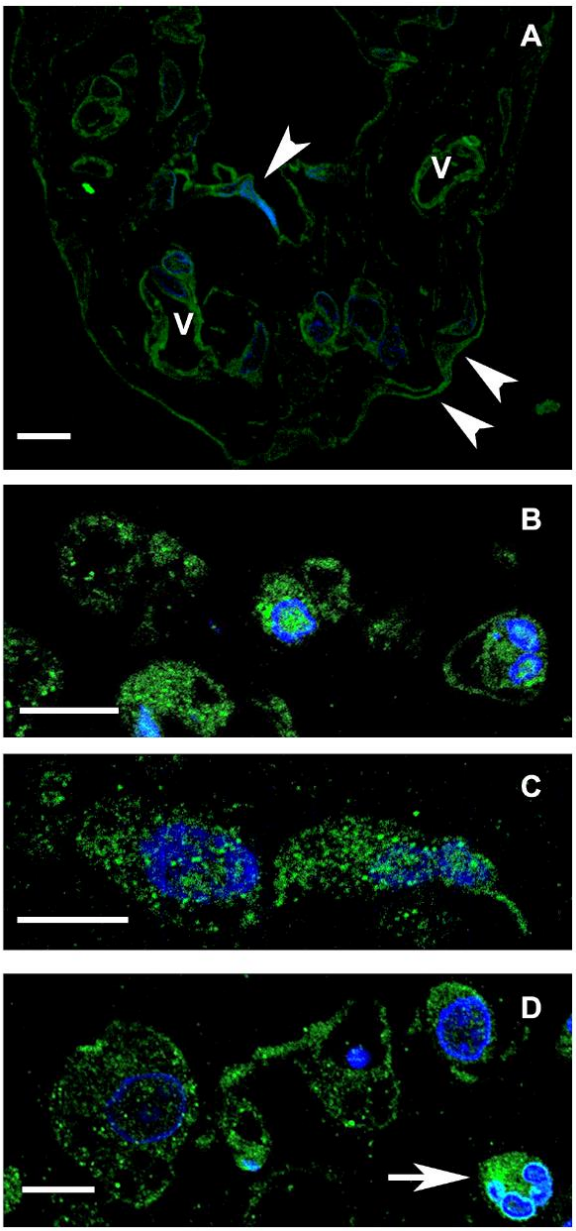

Figure 18. ER-α immunolabeling on control and Freund's adjuvant treated mesothelial cells. **Confocal micrographs of semithin frozen sections**. **A** Mesothelial cells are present on both sides of the connective tissue (white arrowheads). The labeling lines out the contour of mesothelial cells and can be detected in the wall of blood vessels (V) as well. **B-D** Parallel with the rounding up of mesothelial cells the distribution of ER-α becomes better detectable: labeling can be observed in the nucleus, cytoplasm as well as on the plasma membrane both on the second (**B**) and third (**C**) days after treatment. **D** By the fifth day, many of the mesothelial cells express ER-α mostly along the plasma membrane observable as small punctate structures. The connective tissue contains different cell types among which granulocytes express ER-α extensively (white arrow). Nuclei are stained with DAPI (blue). Scale bars: 10μm

DOI:10.14753/SE.2015.1712

5.2.2 The changes in the expression of ER-α upon inflammatory events

To further corroborate the presence of ER-α in mesothelial cells and how its expression changes upon inflammation induction, we measured it both at the mRNA and protein levels. The results of quantitative RT-PCR revealed a significant downregulation of ER-α mRNA expression in mesothelial cells during the progression of inflammation *in vivo* when compared with the control group (Fig. 19 A). (We found the same pattern of changes in the mRNA expression levels of ER-β and G protein-coupled receptor 30, GPR30 as well (data not shown and discussed here.)). However, inconsistent with the RT-PCR results, when we examined the receptor expression levels with Western blot, we found a significant increase of ER-α protein expression between D3 and D5. Further on, between D8 and D11 there was no detectable protein expression (Fig. 19 B).

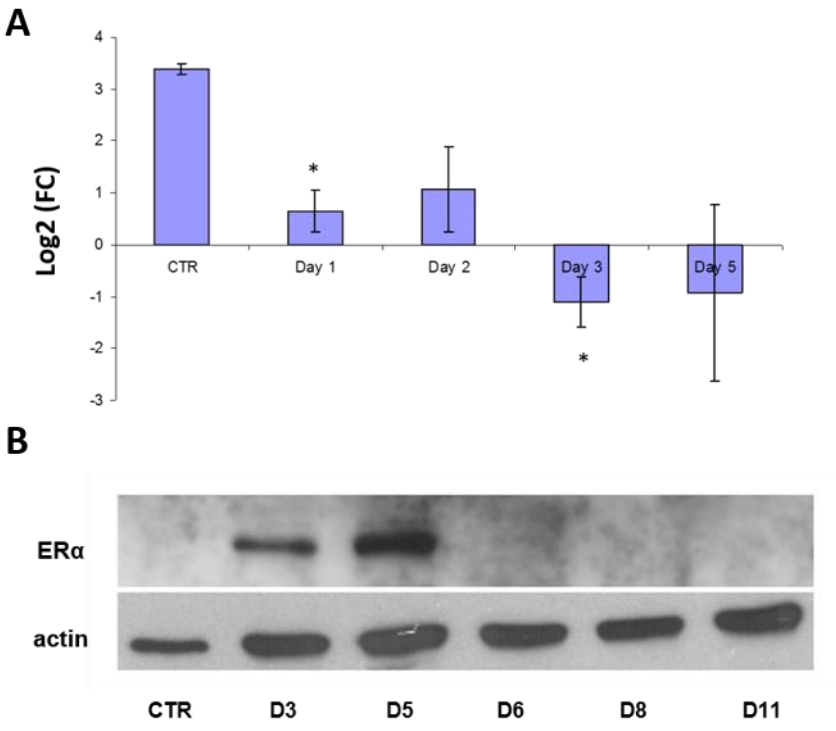

Figure 19. The changes in ER-α expression upon inflammatory events. **A** ER-α mRNA level measured in mesothelial cells is significantly downregulated in response to treatment compared with control group. Asterisks show significant differences from control groups: $p < 0,05$. **B** Western blot analysis using anti ER-α antibody (72 kDa bands) showed a considerable

protein mass between D3 and D5. Afterwards, till D11, there was no detectable protein band. Actin (42 kD) was used in this experiment as control for equal protein loading. One representative of at least four individual replicate experiments is shown.

5.2.3 The intersection of ER-α and TGF-β pathway at the level of caveolae

Since there were controversial data in the literature on the subcellular localization of ER-α in various cell types, we carried out double immunolabeling to detect the fine localization of ER-α as well as their possible co-localization with the coat protein caveolin-1. Our confocal microscopical results show that under inflammatory conditions ER-α colocalized with caveolin-1 both inside the cytoplasm and in the PM (Fig. 20). There were no differences in the distribution of the two markers between D3 and D5 (data not shown). However, in those mesothelial cells that were still attached to the basal membrane, there was a remarkable colocalization of ER-α and caveolin-1 on the luminal surface of the cells (Fig. 20 A). In contrast, with the disintegration of the basal membrane from the third day, ER-α appeared all over the plasma membrane in caveolin-positive membrane domains and colocalization could be detected also inside the cytoplasm (Fig. 20 B). To obtain a more precise view on the localization of ER-α at the ultrastructural level, we carried out immunocytochemistry on ultrathin frozen sections of both non-treated and treated cells. Consistent with the immunofluorescence data, the same distribution of ER-α and caveolin-1 could be found on double-labeled ultrathin frozen sections of treated cells. The immunoelectron microscopic results clearly showed that during the inflammation (D3 and D5) ER-α occurred not only at the plasma membrane but appeared also inside the cytoplasm (Fig. 21 A-B). Here ER-α (together with caveolin-1) was localized in forming or mature MVBs either in their limiting membrane, in association with caveolin-1 or in caveolae, in close vicinity of MVBs (Fig. 21 A-B). In untreated, control mesothelial cells ER-α labeling was accumulated along the plasma membrane on both the luminal and basolateral sides of the cells, preferentially in caveolin-positive vesicles, caveolae (Fig. 21 C). ER-α labeling was also observed inside the nuclei of both untreated and treated mesothelial cells, but to a lesser extent.

DOI:10.14753/SE.2015.1712

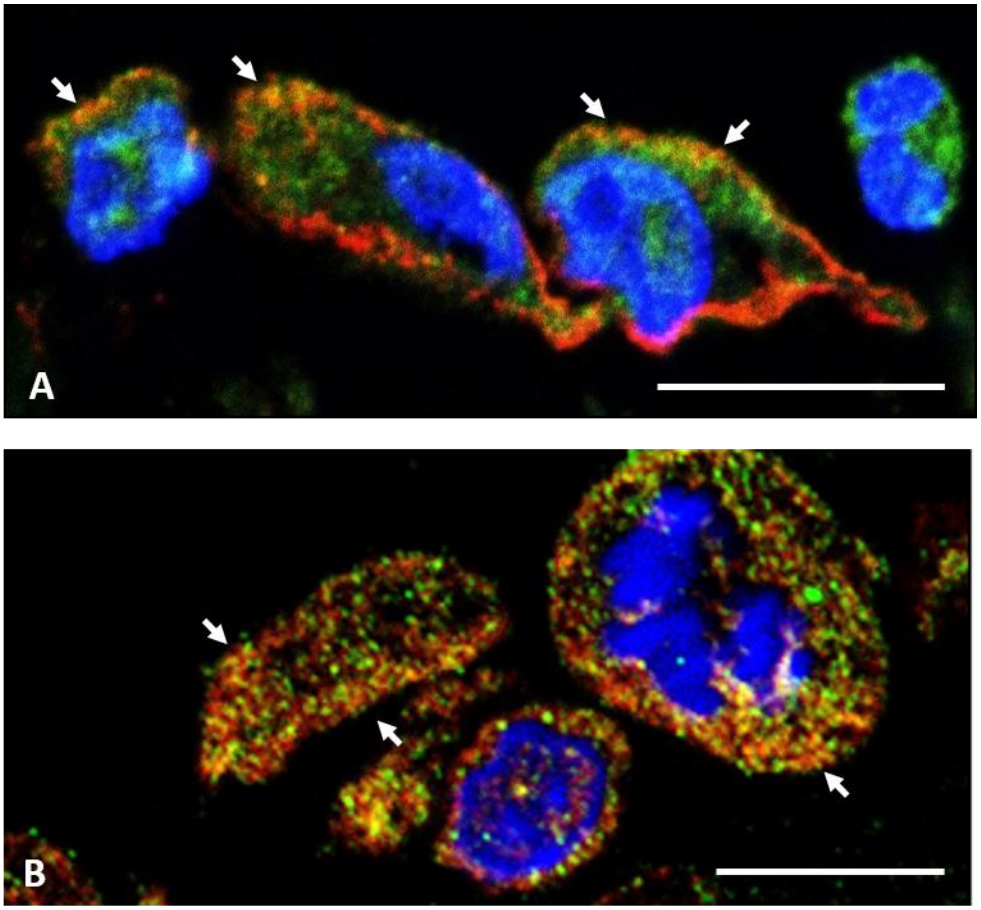

Figure 20. ER-α associates with caveolin-1 and its distribution changes upon inflammatory stimuli. Semithin frozen sections labeled with antibodies against ER-α (green) and caveolin-1 (red). Strong colocalization (orange) could be observed. **A** Two days after treatment, mesothelial cells (still attached to the basal lamina) showed abundant expression of ER-α both inside the cytoplasm as well as at the plasma membrane. The PM ER-α pool accumulated in caveolin-1 positive domains on the luminal side (arrows) of the cells. Less or no green (ER-α) marker could be observed on the opposite side of the cell. **B** In the consecutive day (D3) when cells become apolar and lose contact with the basal lamina, a more intensive co-labeling could be observed over the entire plasma membrane (arrows) with no asymmetric distribution as well as inside the cytoplasm. Nuclei are stained with DAPI (blue) Scale bars: 10μm

DOI:10.14753/SE.2015.1712

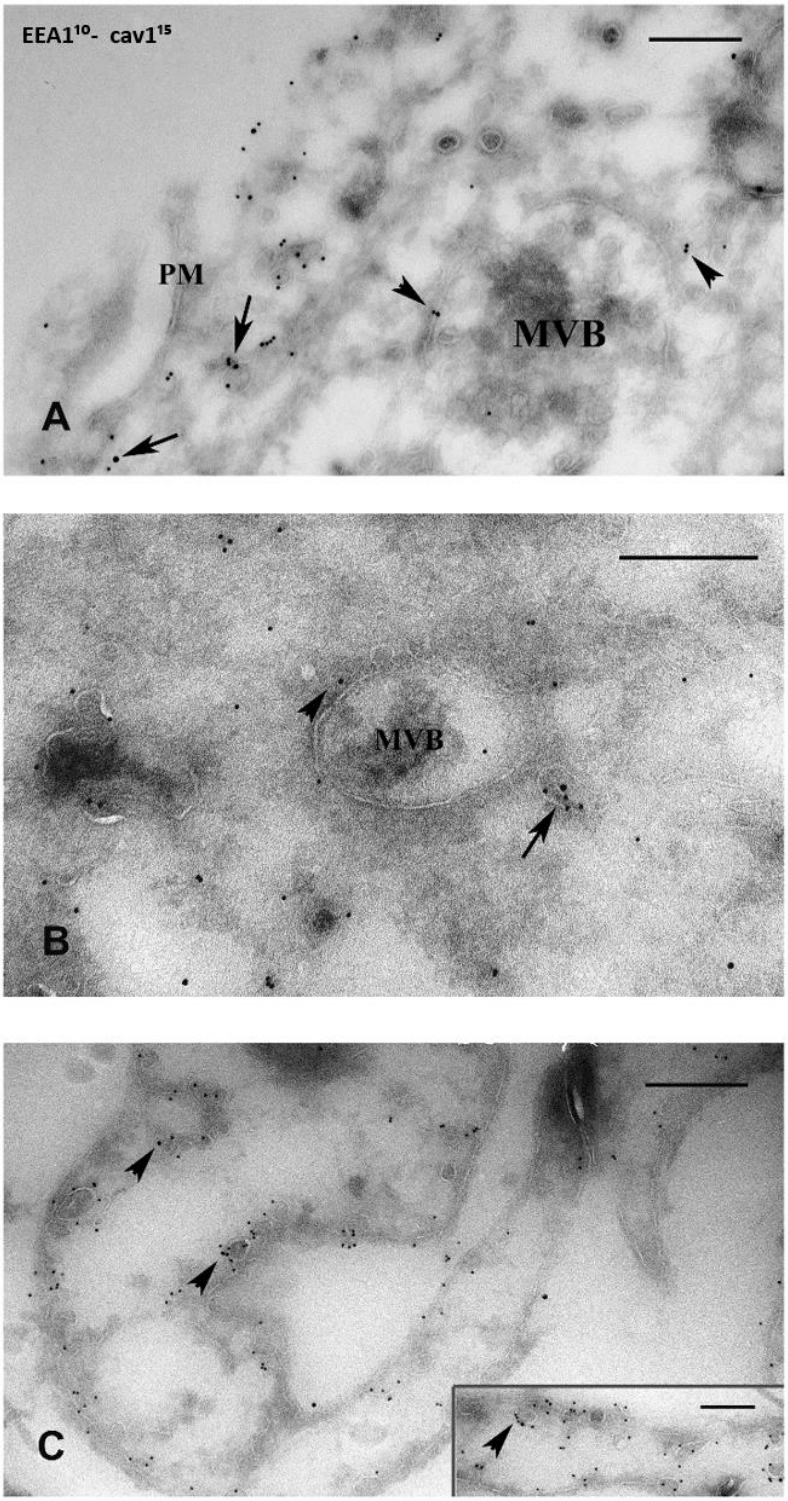

Figure 21. Electron microscopic immunolabeling on ultrathin frozen sections to show ER-α distribution in caveolin-positive lipid rafts and/or caveolae. ER-α was labeled with 15-nm gold particles and caveolin-1 with 10-nm gold. (**A**) ER-α can be found both in the plasma membrane (PM) associated with caveolin-1 (arrows) and (**B**) deeper inside the cytoplasm (arrow) in caveolae upon inflammation. There were no significant differences in the distribution

of ER-α between D3 (**A**) and D5 (**B**). (**A, B**) During multivesicular body (MVB) formation, ER-α was found in the limiting membrane of these organelles and in caveolae in their close vicinity (arrowheads). **C** In non-treated cells ER-α occured in caveolin positive omega-shaped invaginations of the PM. This pattern of the markers was detectable both on the luminal and the basolateral surfaces (arrowheads) in control mesothelial cells. The bars represent (A) 250nm, (B) 400nm (C) 333nm, insert 250nm.

As data from literature described interaction between TGF-β pathway and ER-α, it was another indication to enlighten whether the elements may appear together as the aforementioned morphological results predicted that ER-α and TGF-βRII might use the same internalization route from the peak time of inflammation via caveolae.

For this purpose, we carried out immunofluorescence assay. Our confocal microscopical results showed indeed a remarkable co-labeling between ER-α and TβRII in the cytoplasm of mesothelial cells on D3 samples (Fig. 22 A-C).

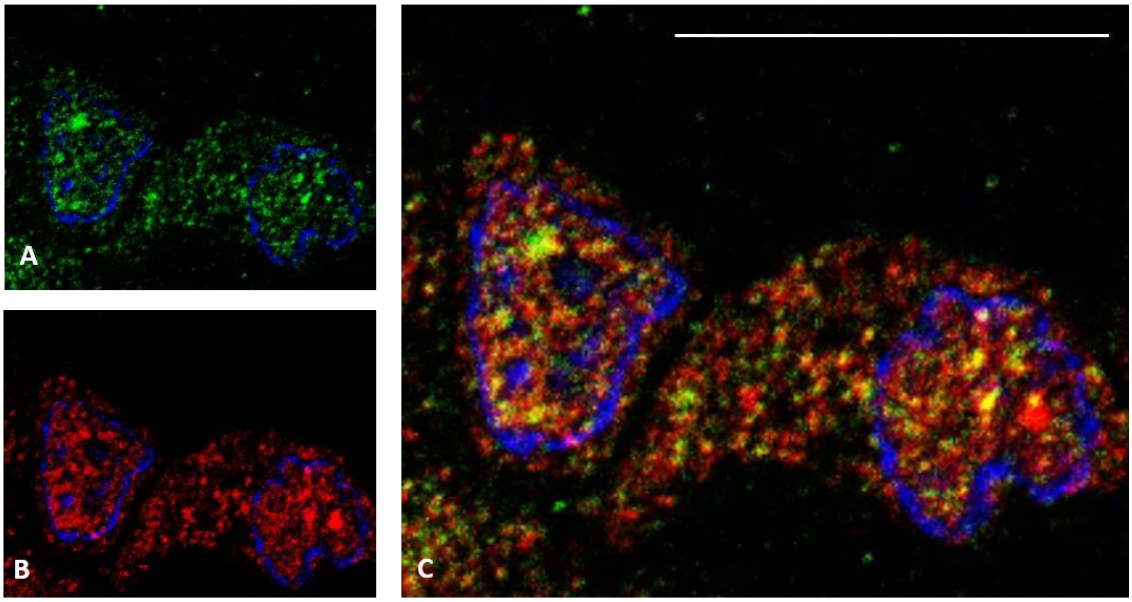

Figure 22. Confocal micrograph showing colocalization between ER-α and TβRII. (C) With the progresison of inflammation, by D3 there were numerous sites inside the cytoplasm where (A) ER-α (green) and (B) TβRII (red) appeared together and colocalized (orange). However, the vast majority of individual ER-α and TβRII labelings appaeared separately. Bar indicates 10μm

DOI:10.14753/SE.2015.1712

5.2.4 Extragonadal estradiol (E2) is detected in the peritoneal cavity under *in vivo* inflammatory circumstances

Since it was shown that ER-α is expressed in mesothelial cells, we were interested in whether there is a natural ligand of the receptor. We measured the hormone levels both in the peritoneal wash and the plasma under control conditions and in response to Freund's adjuvant treatment (induced inflammation) as well. (At least six to eight samples per group were collected in the experiment.) The chemiluminescence assay results revealed that while serum E2 levels remained constantly low at a barely detectable level, there was a striking rise in E2 concentrations measured in the peritoneal fluid. The secreted peritoneal E2 showed a significant peak three days after inducing inflammation and after a moderate decline, following the attenuation of inflammation (between D5 and D11), a prolonged E2 secretion could be observed. This remained markedly higher compared with the control group till D11 (Fig. 23). These results indicated that at this site the observed peritoneal E2 is of extragonadal origin.

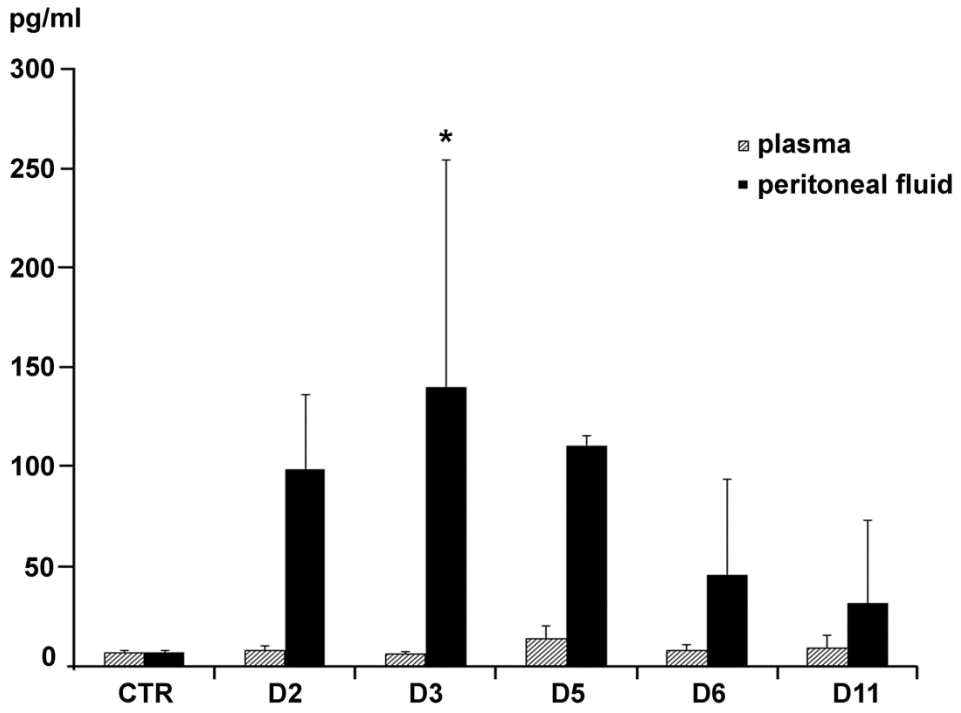

Figure 23. Estradiol concentrations measured in the plasma and peritoneal fluid of male rats upon inflammation induction. There is a significant elevation in the peritoneal E2

concentrations three days after Freund's adjuvant treatment. However a slight decrease could be observed on the consecutive days, but these measured concentrations in the peritoneal wash betwen D5-D11 were stabilized higher when compared with the control samples. The unchanged level in serum E2 concentrations inevitably indicate the presence of locally synthetized, extragonadal E2 hormon. Error bars represent standard deviation, asterisk indicates: $p < 0,05$)

5.3 The role of autophagy in tissue remodelling

5.3.1 The role of autophagy in the retrieval of simple squamous morphology of mesothelial cells following acute inflammation

As sex steroids have been proposed to induce autophagy under inflammatory conditions and we detected a prolonged E2 secretion in our *in vivo* system, our interest turned towards examining whether autophagy is present in mesothelial cells and whether it might contribute to the morphological recovery of mesothelium following inflammation?

Fine structural analysis of mesothelial cells with electron microscopy showed that several double-membrane bound vacuoles engulfing cytosolic structures were present already two to three days after Freund's adjuvant treatment (Fig. 24 A). As the inflammation progressed, by D5 numerous autophage vacuoles were evident in the cytoplasm of mesothelial cells (Fig. 24 B). Frequently, the isolating cistern was only partially formed (Fig. 24 C), but there were matured AVs as well showing myelin configuration (Fig. 24 D). The engulfed structures were recognizable and identified as mitochondria, lipid droplets and endoplasmic reticulum. Further on, the maturation of AVs continued: the inner contents became homogenous in density indicating the ultimate fusion with lysosomes (Fig. 24 E). On D8 samples, the cytoplasm of mesothelial cells were rich in dense lysosome-like structures with several mitochondria also present (Fig. 24 E). By D11, the number of the previously numerous cell organelles in mesothelial cells has been considerably reduced and cells reassumed their flat morphology (Fig. 24 F). Parallel with these notable intracellular changes, the

DOI:10.14753/SE.2015.1712

quantitative analysis also affirmed that the rise in the number of AVs was significant by D5 (Table 2.).

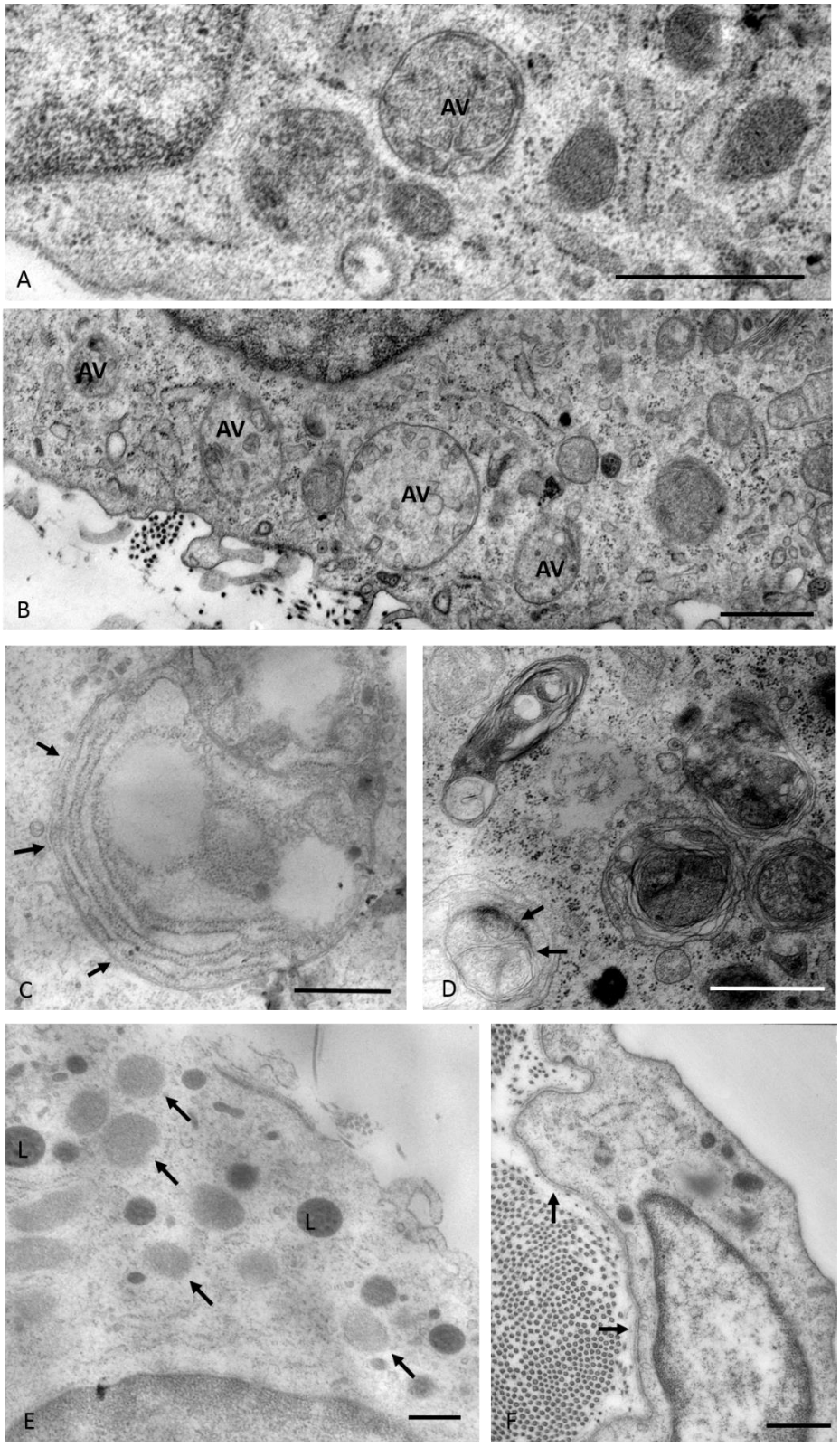

DOI:10.14753/SE.2015.1712

Figure 24. Conventional electron micrographs to show the formation of autophage vacuoles in response to treatment. **A** Two days after treatment, there were autophage vacuoles (AV) already present in mesothelial cells. **B** However, by D5 the cytoplasm were packed with autophage vacuoles (AVs). **C** The double isolating membrane was either partially formed (arrows) or **D** mature AVs surrounded the engulfed material. Observe a mitochondrium (arrows) incorporated into an AV. **E** By D8 several single membrane bounded structures could be identified in the cytoplasm of mesothelial cells that probably represent lysosomes (L). Several less electron dense structures could also be observed in the cytoplasm at this time, presumably mitochondria (arrows) **F** By D11, mesothelial cells regained their flat morphology. Note that the cytoplasm is poor in intracellular organelles. Observe also the continuous basal lamina (arrows) indicating that integrity of the mesothelium has been reestablished. Bars indicate 833nm

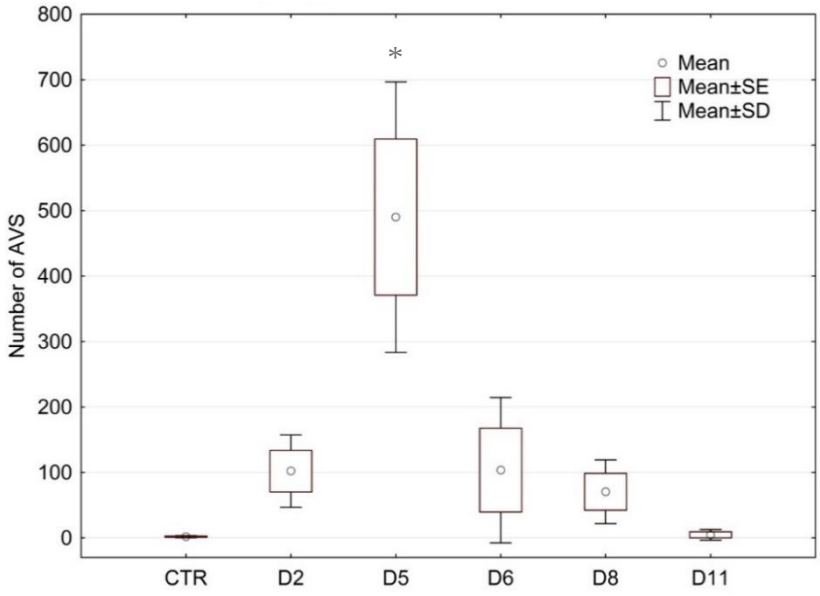

Table 2. The changes in the number of autophage vacuoles in mesothelial cells in response to Freund's adjuvant treatment. The number of autophage vacuoles in correlation with the changes in surface area of mesothelial cells is significantly increased by the fifth day of treatment. (Asterisk: $p<0,05$)

DOI:10.14753/SE.2015.1712

Microtubule-associated protein light chain 3 (LC3) is widely used as a well-validated biomarker of autophagy. Further investigating the protein expression, the Western blot results showed that conversion of LC3-I (inactive form) to LC3-II (active form) was remarkably higher and gradually increased between D5 and D8 indicating that indeed degradative events, the formation of autophage vacuoles was present during the period of regeneration (Fig. 25).

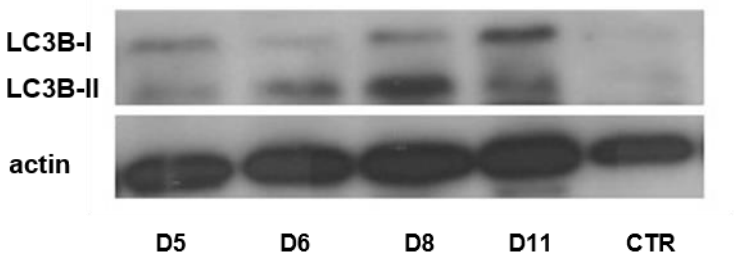

Figure 25. LC3B protein expressions assessed by Western blot. Immunoblotting results show that the expression of LC3B-II (14kDA, active form) protein was upregulated gradually between D5 and D8. One representative of three independent experiments is shown.

5.3.2 The possible inducers of autophagy: Extragonadal estradiol is in the focus

Recent data (Corcelle et al 2007) indicated that estradiol might induce alternative MAPK pathways and enhances autophagy. To assess/rule out the role of E2 in the induction of autophagy, we followed the expression pattern of TNF-α as well that is generally known to contribute to autophagy. The qRT-PCR results show that TNF-α mRNA levels were significantly elevated from D2 after inflammation induction and remained high between D5 and D11 as well (regeneration period) (Fig 26). Estrogen induced autophagosome formation and maturation involves the activation of MAPK pathways such as ERK. Besides this, the involvement of extracellular signal-regulated kinase (Erk) 1/2 in the enhancement of TNF-α induced autophagy is well known. As Erk protein was found as a common mediator of both E2 and TNF-α induced autophagy, we measured the phosphorylation status of this protein in whole cell lysates

of isolated mesothelial cells. Our Western blot results showed that the active (phosphorylated) form of the protein was massively expressed at D6 (Fig 27) during the regenerative period.

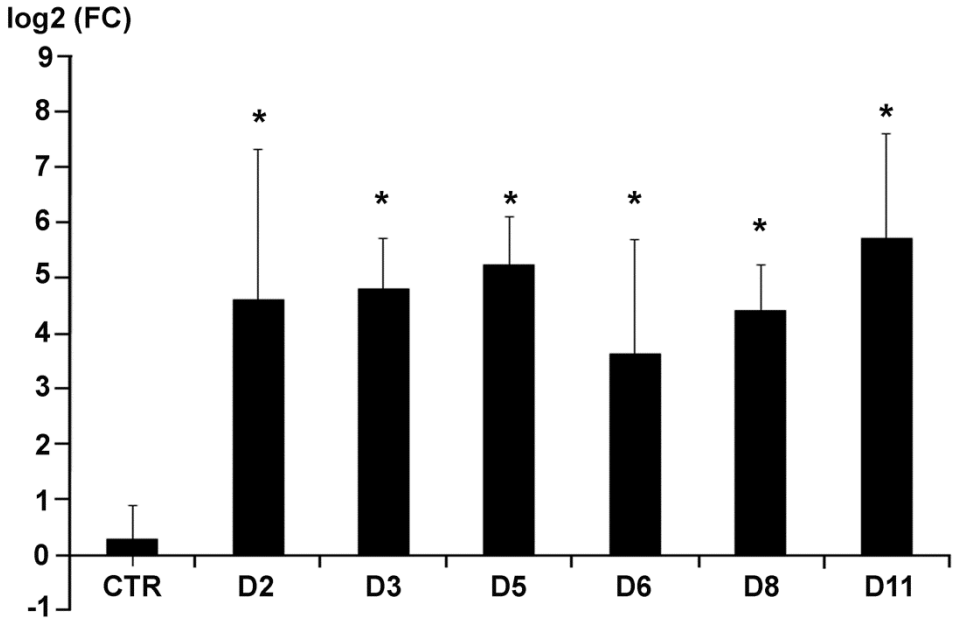

Figure 26. The mRNA expression levels of TNF-α in correlation with Freund's adjuvant treatment and the following regeneration. The expression of TNF-α was upregulated from the early days of inflammation induction and remained high during the regeneration period as well. Error bars represent standard deviation, asterisk indicate: $p<0,05$.

DOI:10.14753/SE.2015.1712

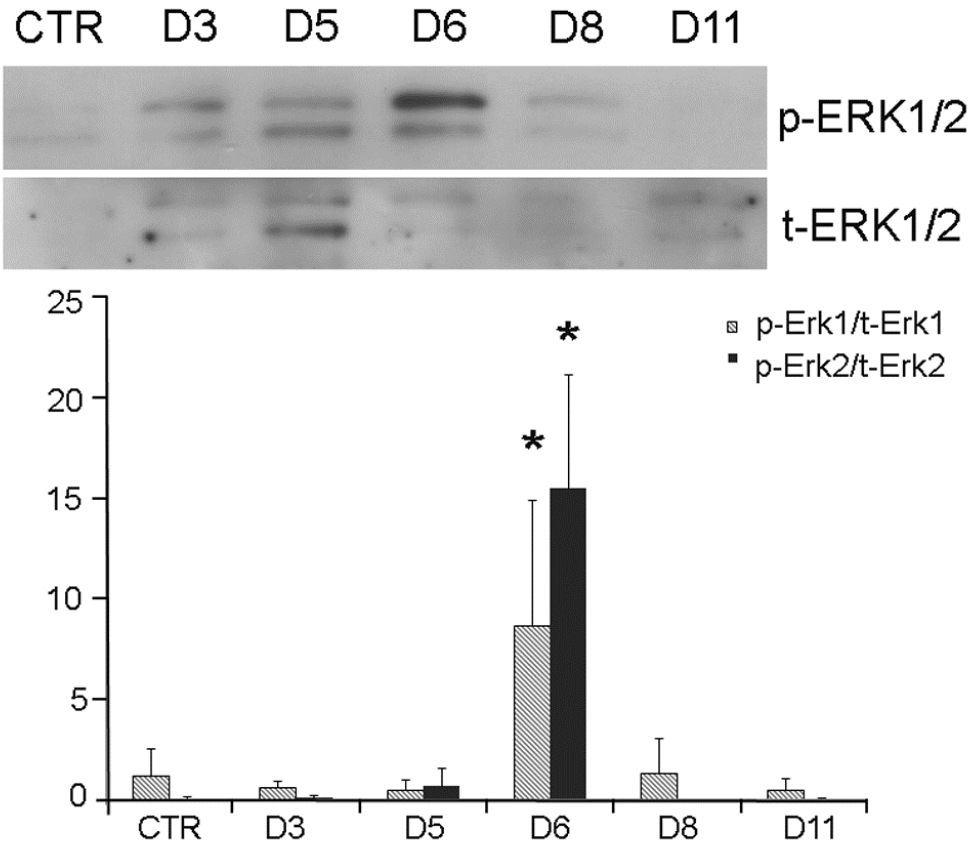

Figure 27. Extracellular signal-regulated kinase (Erk) 1/2 phosphorylation status changes under inflammatory stimuli. Phospho-Erk1/2 (44 and 42 kDa bands) expression levels were detected by using Western blot technique. Massive protein band could be observed at D6. Bars represent standard deviation, asterisks indicate: $p<0,05$.

DOI:10.14753/SE.2015.1712

6. Discussion

Epithelial-mesenchymal transition (EMT) is a complex mechanism that is characterized by a series of events including loss of cell-cell junctions and cell-matrix adhesion, reorganization of cytoskeleton resulting in loss of apical-basolateral polarity and assuming a mesenchymal character such as spindle-shape morphology and locomotion. Due to its role in tumor metastasis as well as in normal embryogenesis and wound healing, the EMT is currently under intensive investigations (Kalluri&Weinberg 2009, Lee et al 2006, Strutz et al 2002). Exploring inflammation-related phenotypic changes (type II EMT) of mesothelial cells specifically and the proteins involved, is of significance since these mechanisms are present in pathological processes of the peritoneum, like in peritoneal dialysis-associated peritonitis (Yanez-Mó et al 2003) and also in local inflammatory processes that might facilitate intraperitoneal cancer metastasis dissemination (Sodek et al 2012).

Our previous light microscopical data revealed how the characteristic molecular markers (cytokeratin, vimentin) of EMT change their expression patterns in mesothelial cells upon inflammatory stimuli induced by Freund's adjuvant treatment (Katz et al 2012). With the present work we aimed to furnish additional evidences for the inflammatory response of the tissue by characterizing the morphological changes at the ultrastructural level as well as to examine the expression levels of pro-inflammatory cytokines (IL 1α, 1β and IL-6) in mesenteric mesothelial cells under *in vivo* circumstances. The disintegration of basal lamina, the loss of polarity by the disassembly of cell-cell junctions, the appearance of spindle-shape morphology observed in mesothelial cells were identical with the steps of EMT described in literature (Kalluri&Weinberg 2009, Lee et al 2006). Besides this, we found a remarkable elevation in the mRNA expression levels of proinflammatory cytokines (IL1a, IL1b, IL6) measured in these cells. This finding further supports the theory that mesothelial cells indeed may contribute to the amplification of inflammatory responses by secreting interleukines and in this way, they are able to play an active role in peritoneal inflammatory events (Offner et al 1995, Douvdevani et al 1994, Topley et al 1993). Proinflammatory cytokines (TNFα, IL1, IL6) are well known to induce immune and inflammatory responses by binding to their receptors. Macrophages are considered

as the major source of proinflammatory cytokines as they produce plethora of these molecules including TNFα, IL-1, IL-6, Il-12, IL-15 and IL-18 (Feldmann&Saklatvala 2001). Macrophages also secrete TGF-β at the site of injury and this cytokine is well known to have a pivotal role in inducing EMT (Kalluri&Weinberg 2009, Lee et al 2006, Strutz et al 2002).

TGF-β is an important morphogenic factor initiating and maintaining EMT via different signaling routes (Smad-dependent, Smad-independent). Besides the canonical Smad-pathway, Smad-independent routes including the Erk, Jnk, p38 MAP kinase cascades are considered to help and complete the process of TGF-β induced EMT. Although there are limited data about the exact mechanisms and biological consequences of these accessory signaling routes, it is apparent that TGF-β induced canonical and non-canonical pathways intersect and both are essential for effective signaling (Lee et al 2007, Kamaraju&Roberts 2005, Moustakas&Heldin 2005, Derynck&Zhang 2003, Engel et al 1999). We also found a significant elevation in the secreted peritoneal TGF-β concentration upon inflammation induction confirming that the cytokine most likely has a role to organize the EMT upon treatment in our *in vivo* system as well.

While the biochemical steps of the canonical Smad-dependent pathway are well characterized, the spatial organization of the events is less elucidated. It has been supported for long that after clathrin-mediated endocytosis the TβR-ligand complex is targeted towards EEA1 positive endosomal compartments (Di Guglielmo 2003). These sites are proved to facilitate the signaling by recruiting FYVE-domain containing proteins such as SARA that helps in the effective phosphorylation of R-Smad proteins (Hayes et al 2002, Penheiter et al 2002). After proving that TGF-β was present in our system, we tried to follow the dynamics of events and examine in detail the compartmentalization of the main canonical TGF-β signaling molecules. Consistent with several reports indicating the central role of early endosomes in the enhancement of signaling, we showed that after internalization TβRII was abundantly present in EEA1 positive cytosolic compartments both under steady state and inflammatory circumstances in mesothelial cells *in vivo*.

There were controversial data about the exact cellular compartments involved in the attenuation of signaling. Besides the possible proteasomal degradation of the receptor,

some reports (Chen 2009, Le Roy&Wrana 2005, Di Guglielmo et al 2003) indicated the negative regulatory role of caveolae in TGF-β signaling. Caveolin-1 is the major protein component of special highly hydrophobic membrane domains, called caveolae. Caveolae are omega-shaped, small plasma membrane invaginations that are found in most mammalian cell types. They play important role in many cellular functions including vesicular transport, endocytosis, transcytosis and are also described to be involved in different signal transduction events (Parton&Simons 2007, Kurzchalia&Parton 1999, Couet et al 1997, Lisanti et al 1995, Lisanti et al 1994). They are likely to provide a platform for clustering signaling molecules. According to literature, Smad7 that is pivotal to terminate TGF-β signaling accumulates in caveolin-1 positive lipid domains of the plasma membrane and acting as a competitive antagonist of R-Smads, it binds the active TβR complex, thus blocking the signal transduction pathway (Di Guglielmo et al 2003, Nakao et al 1997, Hayashi et al 1997). Our light microscopic data were consistent with these findings. Both TβRII as well as negative regulatory protein Smad7 were found to be co-localized with caveolin-1 from the peak time of inflammation that was the critical time when positive signaling turned into attenuation. Degradation of TβRII receptor was further affirmed by the immunoprecipitation results when we found a significant association between TβRII and multivesicular body marker Cd63 three days after treatment.

The most debated and controversial data in the context of regulatory roles of vesicles (early endosomes, caveolae) in TGF-β pathway is whether caveolae directly reach late endosomal compartments (multivesicular bodies/late endosomes) or only with the fusion of early endosomal membranes? Our morphological results obtained both with light as well as with electron microscope provided convincing evidences that caveolae are internalized upon inflammatory stimuli and reach the multivesicular body compartment. This process however requires the involvement of early endosomes. Our immuno-electron micrographs demonstrated that the limiting membrane of forming MVBs were positive for both EEA1 and caveolin-1 markers. The two markers consistently labelled the same limiting membrane, maturing MVB. Hence, indicating not only the fact that caveolae most likely meet the endosomal system at this level, but further affirming that early endosomes are key compartments in the termination of the signaling as well (Katzmann et al 2001). It has already been demonstrated that early

endosomal membrane contains a complex protein machinery, called ESCRT complex that is pivotal for recognizing ubiquitinated cargo proteins and inducing the budding of early endosomal membrane, thus the formation of intraluminal vesicles (ILVs) (Hanson&Cashikar 2012). ILVs are characteristics of multivesicular bodies and the sorting of receptors as well as the proteins targeted for degradation, accumulate within these sites. Fine structural analysis combined with morphometric data proved that at the peak time of inflammation MVB formation was facilitated and not only TβRII but caveolin-1 as well was found to be strongly associated to MVB marker, Cd63. By D5, caveolin-1 showed association with Rab7 that is known to be necessary for the endosomal maturation downstream of multivesicular bodies (Vanlandingham&Ceresa 2009). Collectively, our data strongly support the assumption that caveolin-1 - and cargos associated with caveolin-1 containing lipid domains (caveolae) targeted to lysosomal degradation - unite with classical endocytic pathway at the level of MVB compartments and by decreasing receptor availability, caveola-mediated endocytosis helps in the atteunation of TGF-β singaling.

It has been demonstrated that ER-α has a modulator role in TGF-β signaling, thus can be a potential player in EMT (Band&Laiho 2011). Earlier results from our laboratory have shown that upon adjuvant stimulation mesothelial cells are detached from the basal lamina and assume a macrophage character expressing ED1, a macrophage marker (Katz et al 2011) hence, they can serve as a source of activated macrophages during inflammatory events (Kiss&Kittel 1995). Since macrophages are known to express ER-α (Murphy et al 2009, Straub 2007), the question arose whether treated and untreated mesothelial cells do express ER-α as well? Our present morphological (confocal and immuno-EM) and biochemical (qRT-PCR, Western-blot) results show that ER-α is really present in treated as well as in control mesothelial cells. This finding is of special interest since recently it was shown that in addition to its well known genomic role as a transcription factor ER-α has several non-genomic functions. Nowadays it became generally accepted that a certain amount of ER-α resides in the plasma membrane and is thought to be responsible for inducing both genomic and non-genomic actions by activating different cascades, like PKC, Src kinase, MAPK and PI3K (Levin 2009, Song&Santen 2006, Song et al 2005, Simoncini et al 2004). Our present light microscopic data showed that in parallel with the inflammatory events the

labeling intensity of ER-α was significantly increased and could be detected in the cytoplasm, plasma membrane as well as in the nucleus. Besides the novel finding that ER-α is expressed in mesenteric mesothelial cells, the nuclear pool of the receptor was less pronounced and unchanged during the inflammatory events. This directed our focus to study further the cytoplasmic/plasma membrane pool of ER-α. In mesothelial cells, still in contact with the basal lamina, the distribution of plasma membrane ER-α pool showed a certain polarity with a predominant localization on the luminal side, while after being detached ER-α was distributed all over the plasma membrane. This redistribution of ER-α in the plasma membrane also indicates loss of cell polarity and is a further proof for the transformation of a polarized epithelial cell into a non-polarized mesenchymal cell.

When we measured the mRNA level of ER-α, we found an inverse correlation with the labeling intensity of the protein on our immunocytochemical specimens as well as with the immunoblot results between D3 and D5 demonstrating that on a transcriptional level ER-α was downregulated at this time. Several studies have already described that mRNA and protein levels do not always correlate. The exact mechanism is still unclear, a possible explanation for this phenomenon can be a protein-protein interaction, the altered turnover of the molecule and posttranscriptional regulation by microRNAs (Guttila et al 2012, Jayapal et al 2008, Schmidt et al 2007, Washburn et al 2003).

There are data known from literature showing that ER-α resides in caveolin positive raft compartments of the plasma membrane in many cells (Razandi et al 2002, Driggers&Segards 2002). Our immunocytochemical results also showed that both plasma membrane ER-α and the cytosolic receptor pool were predominantly associated with caveolin-1 protein. As it was previously mentioned, caveolae are involved in several cellular functions and may have role in regulating signaling events and are often considered as ’signaling platforms’ (Parton&del Pozo 2013, Liu et al 1997). These data suggest that caveolae are specific (recruiting) sites of plasma membrane where, besides other transduction proteins, such as TβRII, ER-α is also present. As we followed the intracellular distribution of ER-α, we found that plasma membrane ER-α is internalized upon inflammatory stimuli and is targeted to the classical endosomal pathway - towards multivesicular bodies. This finding is not unusual, since endocytosis of other membrane receptors and their transport along the endosomal pathway have been described in other

signaling systems as well (Di Guglielmo et al 2003, Barbiere et al 2000) (TβRII was found to follow the same route). Caveola-mediated endocytosis presumably helps not only to remove signaling molecules targeted for degradation (TβRII) from the cell surface but also to provide pathway for biologically important signal transducers (ER-α, Src) to reach the proper cytoplasmic platforms (late endosomes, MVBs) where the microenvironment is optimal for their interaction. Considering the colocalization of ER-α with cavolin-1, it is likely that internalization is caveola-mediated. This suggestion is further supported by Christensen et al who also showed that inhibition of Cav-1 by siRNA reduced membrane estrogen-receptor α levels (Christensen&Micevych 2012).

It is known that the association of caveolin-1 and ER-α can activate MAP kinase pathways by interacting either with the signaling proteins or with each other (Song et al 2002, Li et al 1996, Li et al 1995). The best studied interaction in raft domains of the plasma membrane is the induction of ERK pathway through Src/Shc/Grb2/Sos protein complex formation where these proteins physically interact with both caveolin-1 and ER-α and are activated after TGF-β stimulus (Baran et al 2007, Schlegel et al 1999). Taking into consideration these data, we suppose that ER-α might have a role in our system by modifying the activity of the main signaling pathways via maintaining physical interaction with signaling proteins such as caveolin-1 and Src (data not shown).

There are limited data available about the localization of the elements of MAPK cascades inside the cytoplasm. The ERK pathway is well characterized and these studies illustrate the role of endosomal compartments: either the upstream elements of these non-canonical pathways are described to occur in the plasma membrane/membrane of early endosomes or the downstream signaling elements are bound to late endosome/MVB membranes via different adaptor proteins (Zehorai et al 2010, Taub et al 2007, Adachi et al 2000). One of these adaptor proteins (p18) has already been proved to associate with cavolin-1 indicating that upon internalization, the caveolin-1 positive lipid part of endosomal membranes might serve as a recruiting site (Nada et al 2009). They presumably maintain a physical platform to bind the elements of signaling proteins and in this way, they can orchestrate the spatial and temporal regulation of different signaling routes. In this study we showed that ER-α was found either in the limiting membrane of MVBs colocalizing with caveolin-1 or in caveolae in close vicinity to late endosomal/MVB compartments. We hypothesize that the membrane of

endosomal compartments/MVBs can form platforms for molecular clusters and can organize spatial and temporal distribution of signaling proteins. Although our results do not prove directly whether PM ER-α induces signaling from the plasma membrane and whether it controls accessory pathways, however, its association with caveolin-1 and Src (data not shown) strongly suggest that it might play a role in signaling events.

Besides the potential plasma-membrane associated non-genomic effects of ER-α, recent investigations also revealed that ER-α can enhance the degradation of Smad proteins inside the nucleus via ubiquitin-proteasome system and inhibit TGF-β signaling. These data illustrate the role of ER-α as a non-genomic nuclear modifier of TGF-β signaling cascade (Ito et al 2010).

As we showed that ER-α was expressed in mesothelial cells, we were about to demonstrate whether there is a natural ligand of the receptor in the peritoneal cavity. According to the classical belief, ligand binding is essential for effective ER signaling (Nilsson et al 2001, Rosenfeld&Glass 2001), although data is debated about the plasma membrane receptor pool (Song&Sante 2006, Song et al 2005, Wraner&Gustaffson 2006). The natural ligand of ERs, estrogen is considered an important morphogen. Meanwhile the concept about ER receptors has largely changed, the renewal of the theory about their ligand effects was essential as well. Besides their gonadal synthesis some articles reported extragonadal estradiol (E2) production in adipocytes, osteoblasts, chondrocytes, vascular endothelial cells, aortic smooth muscle cells or brain tissue (Bruch et al 1992, Bayard et al 1995, Murakami et al 1998, Labrie et al 1997). Supposingly, the high E2 concentrations achieved at these sites have significant biological effects only *in loco* (Simpson et al 2000, Simpson et al 1999, Labrei et al 1997, Labrie et al 1998). Consistent with this data, our finding also showed that E2 was present in the peritoneal wash under steady state and inflammatory conditions *in vivo*. While the serum hormone levels did not alter during the observed period and were barely detectable, there was a significant elevation of E2 measured in the peritoneal fluid three days after treatment. After a moderate fall the peritoneal E2 concentrations stabilized and showed a prolonged secretion till eleven days after treatment. The source of newly synthesised E2 at these compartments is presumably from androgens converted to estradiol by cytochrome P450 aromatase enzyme. This protein is responsible to bind C_{19} steroids and testosteron and catalyze the formation of estrogen

(Labrie et al 1997, Nelson et al 1996). It has previously been demonstrated that aromatization in the adipose tissue is not negligible under normal and pathological conditions (Vague 1981). Since adipose tissue (adipocytes) is always present in the mesentery along the mesenteric blood vessels, we strongly considered that it has role not only to cushion the vessels but also to maintain a special microenvironment in which activated aromatase enzyme helps in the biosynthesis of estrogen. When we measured the secreted testosteron levels in the peritoneal wash and calculated the E2/T ratios (data not shown), we found a significant correlation in the concentration changes further confirming that aromatase enzyme of the surrounding adipocytes converts testosteron and it serves as the source of the detected extragonadal estradiol in the peritoneal cavity in our system as well.

The detected and prolonged secretion of extragonadal estradiol raised another question: whether it might have a role in tissue regeneration. Among the myriads of factors, sex steroids have recently been described to induce autophagy and help in tissue remodeling (Yang et al 2013, Gajewska et al 2013, Mizushima&Komatsu 2011 Mizushima 2005). Therefore, our interest turned towards examining whether autophagy is present in mesothelial cells following acute inflammation and how the occurrence of AVs might correlate with the E2 secretion changes. Autophagy is characterized by the engulfment of the cell's own cytoplasm and the exfoliation of organelles in double-membrane bound vacuoles results in lysosomal degradation of the content (Levine&Klionsky 2004). We demonstrated here that autophagy was present and was followed by the restitution of simple squamous morphology of mesothelial cells. Using conventional electron microscopy, we found some autophage vacuoles (AVs) even under control conditions but the number of AVs markedly rised five days after treatment. As the regeneration progressed, many autophago-lysosomes, lysosomes and mitochondria were observed. There were no detectable elements of the degradative pathway by the eleventh day after treatment and by this time the morphological re-establishment of the mesothelium was accomplished. Our quantitative analysis also affirmed that the number of AVs markedly rised five days after treatment.

Microtubule-associated protein light chain 3 (LC3) is a widely used and well-validated biomarker of autophagy. The conversion of LC3-I to its active form, LC3-II is a commonly used method to monitor the formatin of AVs. LC3-II is present both in the

inner and outer surfaces of autophagosome membranes and the amount of LC3-II highly correlates with the number of AVs, thus a good indicator of the process (Mizushima&Yoshimori 2007). Our results showed that LC3-II expression gradually increased between D5 and D8 correlating with the excessive number of autophage vacuoles observed during this period and showed also correlation with the prolonged peritoneal E2 concentrations. It is interesting as recent *in vitro* studies suggested that estradiol might upregulate LC3 expression and inducing autophagy, E2 might help in cell survival (Yang et al 2013, Barbati et al 2012)

Autophagosome formation and turnover is precisely regulated by sequential complex events and also involves the activation of MAP kinase pathways such as ERK and p38 pathways that are also well-known estrogen-activated signaling cascades (Corcelle et al 2007). Kinases play an integral role in the inception and execution of autophagy (Shridharan et al 2011). While some kinases such as mTOR, PI3K or AMPK directly regulate the components of autophagic machinery, the precise role of other kinases such as MAPK and protein kinase C in autophagy is less elucidated.

In order to assess or rule out the possible role of E2 in the induction of autophagy *in vivo,* we followed the expression pattern of TNF-α that is known as a general inducer of autophagy (Cheng et al 2008). Measuring the mRNA levels of TNF-α, we found a significant elevation of expression levels even after the inflammation eased (between D5-D11). It has also been proved that macrophage-derived pro-inflammatory cytokines like IL-6 and TNF-α upregulate aromatase expression (Simpson et al 2000). Collectively, it can be assumed that TNF-α most likely contributes not only to induce autophagy but via upregulating aromatase enzyme may support the maintainance of the prolonged E2 secretion in the surrounding adipocytes as well.

Estrogen induced autophagosome formation and maturation involves the activation of MAPK pathways such as Erk (Corcelle et al 2006). Besides this, the involvement of extracellular signal-regulated kinase (Erk) 1/2 in the enhancement of TNF-α induced autophagy is well known. As Erk protein was found as a common mediator of both E2 and TNF-α induced autophagy, we measured the phosphorylation status of this protein and our Western blot results showed that the active (phosphorylated) form of the protein was massively expressed at D6 (period of regeneration).

DOI:10.14753/SE.2015.1712

7. Conclusions

1) we established a type II, inflammation-related EMT model in which the cellular mechanism of the trasformation of mesothelial cells could be examined under *in vivo* circumstances

2) isolating mesothelial cells let us examine from a biochemical point of view the finer cellular changes occurred at the protein and mRNA levels upon inflammation and the following regeneration

3) We showed that inflammatory cytokines and TGF-β were secreted into the peritoneal cavity upon Freund's adjuvant treatment (induced inflammation). The observed ultrastructural changes confirmed that mesothelial cells undergo mesenchymal transition under inflammatory circumstances.

4) we affirmed the presence of TβRII and Smad7 proteins (elements of canonical TGF-β pathway) in mesothelial cells and our morphological observations and biochemical experiments proved that upon inflammation they internalize and reach the degradative pathway. In this process the caveolae and caveolin positive structures played pivotal role

5) our novel finding was that ER-α is expressed in mesenteric mesothelial cells. We found abundant receptor labeling in the plasma membrane of the cells and observed that upon inflammation the receptor pool internalized and reached the degradative pathway via caveola-mediated endocytosis.

6) our present results showed that under *in vivo* inflammatory circumstances extragonadal E2 was secreted into the peritoneal cavity and is most likely contribute to the morphological reestablishment of the mesothelium by promoting autophagy.

7) from the peak time of inflammation and during the regeneration autophagy was present in mesothelial cells and was followed by the appearance of original simple squamous morphology

DOI:10.14753/SE.2015.1712

8. Summary

***Background*:** Epithelial-mesenchymal transition is an important biological process and one of the main organizers of the events is the TGF-β cytokine. Several data indicated the pivotal role of intracellular compartments (endosomes, multivesicular bodies, caveolae) that are capable of modifying the activity of signaling pathways and are also responsible for the spatial organization of signaling molecules. A possible modifier of the canonical TGF-β pathway, thus a potential player in the process of EMT is estrogen-receptor alpha (ER-α). The natural ligand of the receptor, estradiol (E2) was described to be synthesised in several extragonadal sites (adipocytes, brain tissue, aortic smooth muscle cells) and might help in tissue remodelling by promoting autophagy.

Aims: Both morphological and biochemical experiments were applied to follow the subcellular compartmentalization of the molecules of TGF-β pathway and ER-α in inflammation induced EMT. We also examined the possible role of E2 and ER-α in the regeneration period in mesenteric mesothelial cells *in vivo.*

Results: We showed that inflammatory cytokines and TGF-β were secreted into the peritoneal cavity upon Freund's adjuvant treatment (induced inflammation). The observed ultrastructural changes confirmed that mesothelial cells undergo mesenchymal transition under inflammatory circumstances.

We affirmed the presence of TβRII and Smad7 proteins (elements of canonical TGF-β pathway) in mesothelial cells and showed that they internalized and reached the degradative pathway upon inflammation. In this process the caveolae and caveolin positive structures played important role.

Our novel finding was that ER-α was expressed in mesenteric mesothelial cells and was accumulated exclusively in caveolae at the plasma membrane. Upon inflammation the receptor internalized and reached the degradative pathway via caveola-mediated endocytosis.

We also proved that under *in vivo* inflammatory circumstances extragonadal E2 was secreted into the peritoneal cavity and was most likely contributed to the morphological reestablishment of the mesothelium by promoting autophagy.

Conclusion: Our model system is adequate to examine the complex morphological and biochemical changes of EMT at a tissue level, under *in vivo* circumstances. We

DOI:10.14753/SE.2015.1712

confirmed the presence of extragonadal estradiol and its possible role in tissue remodelling, regeneration.

DOI:10.14753/SE.2015.1712

9. Summary in Hungarian (Összefoglalás)

Irodalmi háttér: A hám-mesenchyma átalakulás (EMT) kiemelt fontosságú biológiai folyamat, amelynek egyik fő szabályozója a TGF-β citokin. A TGF-β jelátviteli útvonal aktivitásának szabályozásában a downstream jelátviteli fehérjék sejten belüli eloszlása, különböző kompartimentumokban (korai endoszómák, multivezikuláris testek, caveolák) való lokalizációja kiemelt fontosságú. Irodalmi adatokból ismert, hogy az ösztrogén receptor alfa (ER-α) szerepet játszhat az EMT folyamataiban a kanonikus TGF-β útvonal módosításán keresztül. A receptor természetes ligandja, az ösztrogén extragonadálisan (zsírsejtek, agyszövet, aorta simaizom sejtek) is termelődhet és különböző biológiai folyamatokat (pl. autofágia) indukálhat.

Célkitűzések: Munkánk során morfológiai és biokémiai módszerekkel követtük nyomon a TGF-β jelátviteli útvonal molekuláinak, valamint az ER-α-nak citoplazmatikus eloszlását a gyulladás indukálta hám-mesenchyma átalakulás során. Vizsgáltuk az ösztrogén és ösztrogén receptor alfa (ER-α) lehetséges szerepét a gyulladást követő regeneráció folyamataiban, patkány hashártya mesothel sejtekben *in vivo.*

Eredmények: Igazoltuk, hogy Freund adjuváns kezelés hatására gyulladásos interleukinok termelődnek és a TGF-β nagy mennyiségben szekretálódik a hasüregbe. Ultrastruktúrális vizsgálatokkal igazoltuk, hogy a kezelés hatására a mesothel sejtekben mesenchymális átalakulás megy végbe.

Megállapítottuk, hogy a TGF-β jelátviteli folyamat két fehérjéje (TβRII, Smad7) jelen van mesothel sejtek plazmamembránján, és a gyulladásos reakció második felében a citoplazmatikus eloszlásuk megváltozik: a sejtmembránról korai és késői endoszómákba szállítódnak. Megállapítottuk, hogy a gyulladásos folyamat leállításában, (a TGF-β jelátviteli folyamat leállításában), a jelátviteli molekulák degradatív útvonalra terelésében a caveolák és caveolin-pozitív struktúrák játszanak fontos szerepet.

Bizonyítottuk az ER-α jelenlétét, expressziójának, sejten belüli eloszlásának változását kontroll és gyulladásos folyamatokban. Kimutattuk, hogy a sejtmembránon jelenlévő ER-α mesothel sejtekben szinte kizárólag caveolákban fordul elő, és caveolák közreműködésével internalizálódik.

Igazoltuk, hogy az ösztrogén *in vivo*, kontroll és gyulladásos körülmények között extragonadálisan jelen van a hasüregben, és magas szekréciós szintje a gyulladást

DOI:10.14753/SE.2015.1712

követő regenerációs fázisban, valószínűleg autofágia indukálásán keresztül járul hozzá a mesothel réteg újjászerveződéséhez.

***Konklúzió*:** Modell rendszerünk kiválóan alkalmas az EMT komplex folyamatának *in vivo,* szöveti szintű morfológiai és biokémiai vizsgálatára. Sikerült igazolnunk a klasszikus ösztrogén extragonadális jelenlétét, és lehetséges hatását a gyulladást követő szöveti regenerációban.

10.Bibliography

Adachi M, Fukuda M, Nishida E. (1999) Two co-existing mechanisms for nuclear import of MAP kinase: passive diffusion of a monomer and active transport of a dimer. EMBO J, 18: 5347-5358

Adachi M, Fukuda M, Nishida E. (2000) Nuclear export of MAP kinase (Erk) involves a MAP kinase kinase (MEK)-dependent active transport mechanism. J Cell Biol, 148: 849-856

Balogh P, Katz S, Kiss AL. (2013) The role of endocytic pathways in TGF-β signaling. Pathol Oncol Res, 19: 141-148

Balogh P, Szabó A, Katz S, Likó I, Patócs A, Kiss AL. (2013) Estrogen receptor alpha is expressed in mesenteric mesothelial cells and is internalized in caveolae upon Freund's adjuvant treatment. PLoS One, (11) p. e79508. 10 p.

Band AM, Laiho M. (2011) Crosstalk of TGF-β and estrogen receptor signaling in breast cancer. J Mammary Gland Biol Neoplasia, 16: 109-115

Baran J, Mundy ID, Vasanji A, Parat MO. (2007) Altered localization of H-Ras in caveolin-1-null cells is palmitoylation-independent. J Cell Commun Signal, 1: 195-204

Barbati C, Pierdominici M, Gambardella L, LbediMF, Karas HR, Rosano G, Malorni W, Ortona E. (2012) Cell surface estrogen receptor alpha is upregulated during subchronic metabolic stress and inhibits neuronal cell degeneration. PLoS One, DOI: 10.1371/journal.pone.0042339

Barbiere MA, Roberts RL Gumusboga A, Highfield H, Alvarez-Domingez C, Wells A, Stahl PD. (2000) Epidermal growth factor and membrane trafficking. EGF receptor activation of endocytosis requires Rab5a. J Cell Biol, 151: 539-550

Bayard F, Clamens S, Delsol G, Blaes N, Maret A, Faye JC. (1995) Oestrogen biosynthesis, oestrogen metabolism and functional oestrogen receptors in bovine aortic endothelial cells. Ciba Foundation Symposia, 19: 122-132.

Beato M, Herrlich P, Schutz G. (1995) Steroid hormon receptors: many actors insearch of a plot. Cell, 83: 851-857

Bizet AA, Liu K, Tran- Khanh N, Saksena A, Vorstenbosch J, Finnson KW, Buschmann MD, Philip A. (2011) The TFG-β co-receptor, CD109, promotes internalization and degradation of TGF-β receptors. Biochim Biophys Acta, 1813: 742-53.

Bonifacino JS, Lippincott-Schwartz J. (2003) Coat proteins: shaping membrane transport. Nat Rev Mol Cell Biol, 4: 409-14.

Bonifacino JS, Traub LM. (2003) Signals for sorting of transmembrane proteins to endosomes and lysosomes. Annu Rev Biochem, 72: 395-447.

Bradford MM. (1976) A rapid and sensitive method for the quantitation of microgram quantities of protein utilizing the principle of protein-dye binding. Anal Biochem, 72: 248-54

Bruch HR, Wolf L, Budde R, Romalo G, Schweikert HU. (1992) Androstenedione metabolism in cultured human osteoblast-like cells. J Clin Endocrin Metab, 75: 101-105.

Chen RH, Sarnecki C, Blenis J. (1992) Nuclear localization and regulation of erk- and rsk-encoded protein kinase. Mol Cell Biol, 12: 915-927

Chen YG. (2009) Endocytic regulation of TGF-β signaling. Cell Res, 19:58-70.

Chen YG, Wang Z, Ma Y, Zhang L, Lu Z. (2007) Endofin, a FYVE domain protein, interacts with Smad4 and facilitates transforming growth factor-beta signaling. J Biol Chem, 282: 9688-96

Cheng Y, Qiu F, Tashiro S, Onodera S, Ikejima T. (2008) ERK and JNK mediate TNFalpha-induced p53 activation in apoptotic and autophagic L929 cell death. Biochem Biophys Res Commun, 376: 483-488

Choi AJS, Ryter SW. (2011) Autophagy in inflammatory diseases. Int J Cell Biol, doi:10.1155/2011/732798

Christensen A, Micevych P. (2012) CAV1 siRNA reduces membrane estrogen receptor-alpha levels and attenuates sexual receptivity. Endocrinology, 153: 3872-3877

Chuderland D, Seger R. (2005) Protein-protein interactions in the regulation of the extracellular signal-regulated kinase. Mol Biothechnol, 29: 57-74

Ciechanover A. (2005) Proteolysis: from the lysosome to ubiquitin and the proteasome. Mol Cel Biol, 6: 79-86

Corcelle E, Djerbi N, Mari M, Nebout M, Fiorini C, Fénichel P, Hofman P, Poujeol P, Mograbi B. (2007) Control of the autophagy maturation step by the MAPK ERK and p38: lessons from environmental carcinogens. Autophagy, 3: 57–59.

Corcelle E, Nebout M, Bekri S, Gauthier N, Hofman P, Poujeol P, Fenichel P, Mograbi B. (2006) Disruption of autophagy at the maturation step by the carcinogen lindane is associated with the sustained mitogen-activated proein kinase/extracellular signal-regulated kinase activity. Cancer Res, 66: 6861-6870

Couet J, Li S, Okamoto T, Scherer P, Lisanti MP. (1997) Molecular and cellular biology of caveolae: Paradoxes and plasticities. Trends Cardiovasc Med, 7: 103-110

Derynck R, Zhang YE. (2003) Smad-dependent and Smad-independent pathways in TGF-β family signalling. Nature, 424: 577- 584

Di Guglielmo GM, Le Roy C, Goodfellow AF, Wrana L. (2003) Distinct endocytic pathways regulate TGF-β receptor signalling and turnover. Nat Cell Biol, 5: 410-21.

Douvdevani A, Rapoport J, Konforty A, Argov S, Ovnat A, Chaimovitz C. (1994) Human peritoneal mesothelial cells synthesize IL-1α and β. Kidney Int, 46: 993-1001

Driggers P, Segards JH. (2002) Estrogen action and cytoplasmic signaling pathways. Part II: The role of growth factors and phosphorylation in estrogen signaling. Trends Endocrinol Metab, 13: 422-427

Ebisawa T, Fukuchi M, Murakami G, Chiba T, Tanaka K, Imamura T, Miyazono K. (2001) Smurf1 interacts with transforming growth factor-beta type-I receptor through Smad7 and induces receptor degradation. J Biol Chem, 276: 12477-80.

Engel M, McDonnell MA, Law BK, Moses HL. (1999) Interdependent Smad and JNK signaling in trasforming growth factor-β-mediated transcription. J Biol Chem, 274: 37413-37420

Felder S, Miller K, Moshren G, Ullrich A, Schlessinger J, Hopkins CR. (1990) Kinase activity controls the sorting of the epidermal growth factor receptor within the multivesicular body. Cell, 61: 623-34.

Feldmann M, Saklatvala J. (2001) Proinflammatory cytokines. In: Oppenheim JJ & Feldman M, eds. Cytokine Reference. New York: Academic Press 291-305

Fukuda M, Gotoh I, Gotoh Y, Nishida E. (1996) Cytoplasmic localization of MAP kinase kinase directed by its N-terminal, leucine-rich short amino acid sequence, which acts as a nuclear export signal. J Biol Chem, 271: 20024-20028

Fukuda M, Gotoh Y, Nishida E. (1997a) Interaction of MAP kinase with MAP kinase kinase: its possible role in the control of nucleocytoplasmic transport of MAP kinase. EMBO J, 16: 1901-1908

Gajewska M, Zielniok K, Motyl T: Autophagy in development and remodelling of mammary gland. In : Yannick Bailly (editor) Autophagy – A double-edged sword-cell survival or death? InTech 2013 Chapter 20

Galliher AJ, Schiemann WP. (2007) Src phosphorylates Tyr284 in TGF-β type II receptor and regulates TGF-β stimulation of p38 MAPK during brest cancer cell proliferation and invasion. Cancer Res, 67: 3752-3758

Galmiche A, Fueller J, Santel A, Krohne G, Witting I, Doye A, Rolando M, Flatau G, Lemichez E, Rapp ÚR. (2008) Isoform-specific interaction of C_RAF with mitochondria. J Biol Chem, 283: 14857-14866

Gillooly DJ, Simonsen A, Stenmark H. (2001) Cellular functions of phosphatidylinositol 3-phosphate and FYVE domain proteins. Biochem J, 355: 249-58.

Gruenberg J, Maxfield F. (1995) Membrane transport in the endocytic pathway. Curr Op Cell Biol, 7: 552-63.

Guttila IK, Adams BD, White BA. (2012) ERα, microRNAs, and the epithelial-mesenchymal transition in breast cancer. Trends Endocrinol Metab, 23: 73-82

Guttilla IK, Phoenix KN, Hong X, Tirnauer JS, Claffey KP, White BA. (2012) Prolonged mammosphere culture of MCF-7 cells induces an EMT and repression of the estrogen receptor by microRNAs. Breast Cancer Res Treat, 132: 75-85

Hall JM, Couse JF, Korach K. (2001) The multifaceted mechanisms of estradiol and estrogen receptor signaling. J Biol Chem, 276: 36869-36872

Hanson PI, Cashikar A. (2012) Multivesicular body morphogenesis. Annu Rev Cell Biol, 28:337-362

Hay ED. (2005) The mesenchymal cell, its role in the embryo, and the remarkable signaling mechanisms that create it. Dev Dyn, 233: 706-720

Hayashi H, Abdollah S, Qui Y, Cai J, Xu JJ, Grinnell BW, Richardson MA, Topper JN, Gimbrone MAJr, Wrana JL? Falb D. (1997) The MAD-related protein Smad7 associates with the TGFbeta receptor and functions as an antagonist of TGFbeta signaling. Cell, 89: 1165-73.

Hayer A, Stoaber M, Ritz D, Engel S, Meyer HH, Helenius A. (2010) Caveolin-1 is ubiquitinated and targeted to intraluminal vesicles in endolysosomes for degradation. J Cell Biol,191: 615-29.

Hayes S, Chawla A, Corvera S. (2002) TGFβ receptor internalization into EEA1-enriched early endosomes: role in signaling to Smad2. J Cell Biol, 158: 1239-49.

Heldin CH, Moustakas A. (2012) Role of Smads in TGFβ signaling. Cell Tissue Res, 347: 21-36.

Ito I, Hanyu A, Wayama M, Goto N, Katsuno Y, Kawasaki S, Nakajima Y, Kajiro M, Komatsu Y, Fujimura A, Hirota R, Murayama A, Kimura K, Imamura T, Yanagisawa J. (2010) Estrogen inhibits transforming growth factor β signaling by promoting Smad2/3 degradation. J Biol Chem, 285: 14747-55.

Itoh F, Divecha N, Brocks L, Brocks L, Oomen L, Janssen H, Calafar J, Itoh S, Dijke PtP. (2002) The FYVE domain in Smad anchor for receptor activation (SARA) is sufficient for localization of SARA in early endosomes and regulates TGF-beta/Smad signalling. Genes Cells, 7: 321-31.

Itoh S, Landström M, Hermansson A, Itoh F, Heldin CH, Heldin NE, Dijke PtP. (1998) Transforming growth factor beta1 induces nuclear export of inhibitory Smad7. J Biol Chem, 273: 29195-201.

Jayapal KP, Philp RJ, Kok YJ, Yap MGS, Sherman DH, TJ Griffin, WS Hu. (2008) Uncovering genes with devergent mRNA-protein dynamics in Streptomyces coelicolor. PLoS ONE, 3: e2097

Kalluri R, Weinberg RA. (2009) The basics of epithelial-mesenchymal transition. J Clin Invest, 119: 1420-28.

Kamaraju AK, Roberts AB. (2005) Role of Rho/ROCK and p38 MAP kinase pathways in transforming growth factor-β-mediated Smad-dependent growth inhibition of human breast carcinoma cells in vivo. J Biol Chem, 280: 1024-1036

Kang JS, Liu C, Derynck R. (2009) New regulatory mechanisms of TGF-β receptor function. Trends Cell Biol, 19: 385-394

Katz S, Balogh P, Kiss AL. (2011) Mesothelial cells can detach from the mesentery and differentiate into macrophage-like cells. APMIS, 119: 782-793

Katz S, Balogh P, Nagy N, Kiss AL. (2012) Epithelial-to-mesenchymal transition induced by Freund's adjuvant treatment in rat mesothelial cells: a morphological and immunocytochemical study. Pathol Oncol Research, 18: 641-649

Katzmann DJ, Babst M, Emr DS. (2001) Ubiquitin-dependent sorting into the multivesicular body pathway requires the function of a conserved endosomal protein sorting complex, ESCRT-I. Cell, 106: 145-55.

Kavsak P, Rasmussen RK, Causing CG, Bonni S, Zhu H, Thomsen GH, Wrana JL. (2000) Smad7 binds to Smurf2 to form an E3 ubiquitin ligase that targets the TGF-beta receptor for degradation. Mol Cell, 6: 1365-75.

Kiss AL, Botos E. (2009) Endocytosis via caveolae: alternative pathway with distinct cellular compartments to avoid lysosomal degradation? J Cell Mol Med, 13: 1228-37.

Kiss AL, Kittel A. (1995) Early endocytotic steps in elicited macrophages: omega-shaped plasma membrane vesicles at their cell surface. Cell Biol Int, 19: 527-538

Klionsky DJ. (2007) Autophagy: from phenomenology to molecular understanding in less than a decade. Nat Rev Mol Cell Biol, 8: 931-937
Klionsky DJ, Abdalla FC, Abeliovich H et al. (2012) Guidelines for the use and interpretation of assays for monitoring autophagy. Autophagy, 8: 445-544

Kowanetz M, Lönn P, Vanlandewijck M, Kowanetz K, Heldin CH, Moustakas A. (2008) TGFbeta induces SIK to negatively regulate type I receptor kinase signaling. J Cell Biol, 182: 655-62.

Kretzschmar M, Doody J, Timokhina I, Massagué J. (1999) A mechanism of repression of TGF-β/Smad signaling by oncogenic Ras. Genes Dev, 13: 804-816

Kroemer G, Marino G, Levine B. (2010) Autophagy and the integrated stress response. Mol Cell, 40: 280-293

Kurisaki A, Kose S, Yoneda Y, Heldin CH, Moustakas A. (2001) Transforming growth factor-beta induces nuclear import of Smad3 in an importin-beta1 and Ran-dependent manner. Mol Biol Cell, 12: 1079-91.

Kurzchalia TV, Parton RG. (1999) Membrane microdomains and caveolae. Curr Opin Cell Biol, 11: 424-431

Labrie F, Belanger A, Cusan L, Candas B. (1997) Physiological changes in dehydroepiandrosterone are not reflected by serum levels of active androgens and estrogens but of their metabolites: intracrinology. J Clin Endocrinol Metab, 82: 2403-2409

Labrie F, Belanger A, Cusan L, Gomez JL, Candas B. (1997) Marked decline serum concentrations of adrenal C19 sex steroid precursors and conjugated androgen metabolites during aging. J Clin Endocrinol Metab, 82: 2396-2402

Labrie F, Belanger A, Luu-The V, Labrie C, Simond J, Cusan L, Gomez JL, Candas B. (1998) DHEA and the intracrine formation of androgens and estrogens in peripheral target tissues: its role during aging. Steroids, 63: 322-328

Le Roy C, Wrana L. (2005) Clathrin- and non-clathrin- mediated endocytic regulation of cell signalling. Nat Rev Cell Biol, 6: 112-126.

Lee JA. (2012) Neuronal autophagy: a housekeeper or a fighter in neuronal cell survival? Exp Neurobiol, 21: 1-8

Lee MJ, Dedhar S, Kalluri R, Thompson WE. (2006) The epithelial-mesenchymal transition: new insights in signaling, development, and disease. J Cell Biol, 172: 973-981

Lee MK, Pardoux C, Hall MC, Lee PS, Warburton D, Qing J, Smith SM, Derynck R. (2007) TGF-β activates Erk MAP kinase signaling through direct phosphorylation of ShcA. EMBO J, 26: 3957-3967

Levin ER. (2002) Cellular functions of plasma membrane estrogen receptors. Steroids, 67: 471-475

Levin ER. (2009) Plasma membrane estrogen receptors. Trends Endocrinol Metab, 20: 477-82

Levine B, Klionsy DJ. (2004) Development by self-digestion: molecular mechanisms and biological functions of autophagy. Dev Cell, 6: 463-477

Levine B, Kroemer G. (2008) Autophagy in the pathogenesis of disease. Cell, 132: 27-42

Levine B, Mizushima N, Virgin HW. (2011) Autophagy in immunity and inflammation. Nature, 469: 323-335

Li S, Couet J, Lisanti MP. (1996) Src tyrosine kinases, Galpha subunits, and H-Ras share a common membrane-anchored scaffolding protein, caveolin. Caveolin binding negatively regulates the auto-activation of Src tyrosine kinases. J Biol Chem, 271: 29182-29190

Li S, Okamoto T, Chun M, Sargiacomo M, Casanova JE, Hansen SH, Nishimoto I, Lisanti MP. (1995) Evidence for a regulated interaction between heterotrimeric G proteins and caveolin. J Biol Chem, 270: 15693-15701

Lisanti MP, Scherer P, Tang ZL, Sargiacomo M. (1994) Caveolae, caveolin and caveolin-rich membrane domains: a signalling hypothesis. Trends Cell Biol, 4: 231-235.

Lisanti MP, Tang Z, Scherer PE, Kübler E, Koleske AJ, Sargiacomo M. (1995) Caveolae, transmembrane signalling and cellular transformation. Mol Membr Biol, 12: 121-124

Liu J, Oh P, Horner T, Rogers RA, Schnitzer JE. (1997) Organized endothelial cell surface signal transduction in caveolae distinct from glycosylphosphatidylinositol-anchored protein microdomains. J Biol Chem, 272: 7211-7222

M Yanez-Mó, Lara-Pezzi E, Selgas R, Ramírez-Hueasca M, Domingez-Jimenez C, et al. (2003) Peritoneal Dialysis and Epithelial-to-Mesenchymal Transition of Mesothelial Cells. N Eng J Med, 348: 403-413

Massagué J. (1998) TGF-β signal transduction. Annu Rev Biochem, 67: 753-91.

Mauvais-Jarvis F. (2012) Estrogen sulfotransferase: Intracrinology meets metabolic diseases. Diabetes, 61: 1353-54

Migliaccio A, Di Domenico M, Castoria G, de Falco A, Bontempo B, Nola E, Auricchio F. (1996) Tyrosine kinase/p21 ras/MAP-kinase pathway activation by estradiol-receptor complex in MCF-7 cells. EMBO J, 15: 1292-1300

Mitchell H, Choudhury A, Pagano RE, Leof EB. (2004) Ligand-dependent and –independent transforming growth factor-beta receptor recycling regulated by clathrin-mediated endocytosis and Rab11. Mol Biol Cell, 15: 4166-78.

Mizushima M, Yoshimori T. (2007) How to interpret LC3 immunoblotting. Autophagy, 3: 542-545

Mizushima N. (2005) The pleitotropic role of autophagy: from protein metabolism to bactericide. Cell Death Differ, 12 Suppl 2: 1535-1542

Mizushima N. (2007) Autophagy: process and function. Genes Dev, 21: 2861-2873

Mizushima N, Komatsu M. (2011) Autophagy: Renovation of cells and tissues. Cell, 147: 728-741

Mizushima N, Levine B, Cuervo AM, Klionsky DJ. (2008) Autophagy figths disease through cellular self-digestioin. Nature, 451: 1069-1075

Mori S, Matsuzaki K, Yoshida K, Furukawa F, Tahashi Y, Yamagata H, Sekimoto G, Seki T, MAtsui H, Nishizawa M, Fujisawa J, Okazaki K. (2004) TGF-β and HGF transmit the signals through JNK-dependent Smad2/3 phosphorylation at the linker region. Oncogene, 23: 7416-7429

Morris PG, Hudis CA, Giri D, Morrow M, Falcone DJ, Zhou XK, Du B, Brogi E, Crawford CB, Kopelovich L, Subbaramaiah K, Dannenberg AJ. (2011) Inflammation

and increased aromatase expression occur in the breast tissue of obese women with breast cancer. Cancer Prev Res, 4: 1021-1029

Moustakas A, Heldin CH. (2005) Non-Smad TGF-β signals. J Cel Sci, 118: 3573-3584

Moustakas A, Souchelnytskyi S, Heldin CH. (2001) Smad regulation in TGF-β signal transduction. J Cell Sci, 11: 4359-69.

Mukhopadhyay D, Riezman H. (2007) Proteasome-independent functions of ubiquitin in endocytosis and signaling. Science, 315: 201-205

Murakami H, Sasano H, Satoh A, Satomi S, Nagura H, Harada N. (1998) Aromatase in human aortic tissue. 79th Annual Meeting of the Endocrine Society, Minneapolis, MN, USA p212 (Abstract)

Murphy AJ, Guyre PM, Wira CR, Piolo PA. (2009) Estradiol regulates expression of estrogen receptor ERα46 in human macrophages. PLoS ONE, 4: e5539

Nada S, Hondo A, Kasai A, Koike M, Saito K, Uchiyama Y, Okada M. (2009) The novel lipid raft adaptor p18 controls endosome dynamics by anchoring the MEK-ERK pathway to late endosomes. EMBO J, 28: 477-489

Nakao A, Afrakhte M, Moren A, Nakayama T, Christian JL, Heuchel R, Itoh S, Kawabata M, Heldin NE, Heldin CH, Dijke PtP. (1997) Identification of Smad7, a TGF-beta inducible antagonist of TGF-beta signalling. Nature, 389: 631-35.

Nelson DR, Koymans L, Kamataki T, Stegeman JJ, Feyereisen R, Waxman DJ, Waterman MR, Gotoh O, Coon MJ, Estabrook RW, Gunsalus IC, Nebert DW. (1996) P450 superfamily: update on new sequences, gene mapping, accession numbers and nomenclature. Pharmacogenetics, 6: 1-42

Nicols BJ. (2002) A distinct class of endosome mediates clathrin- independent endocytosis to the Golgi complex. Nat Cell Biol, 4: 374-78.

Nilsson S, Makela S, Treuter E, Tujague M, Thomsen J, Andersson G, Enmark E, Pettersson K, Warner M, Gustafsson JA. (2001) Mechanism of estrogen action. Physiol Rev, 81: 1535-1565

Offner FA, Obrist P, Stadlmann S, Feichtinger H, Klinger P, et al. (1995) IL-6 secretion by human peritoneal mesothelial and ovarian cancer cells. Cytokine, 7: 542-547

Ohsumi Y. (2001) Molecular dissection of autophagy: two ubiquitin-like systems. Nat Rev Mol Cell Biol, 2: 211-216

Parton G, Howes MT. (2010) Revisiting caveolin trafficking: the end of the caveosome. J Cell Biol, 191: 439-441

Parton RG, del Pozo MA. (2013) Caveolae as plasma membrane sensors, protectors and organizers. Nat Rev Mol Cell Biol, 14: 98-112

Parton RG, Howes MT. (2010) Revisiting caveolin trafficking: the end of the caveosome. J Cell Biol, 191: 439-441

Parton RG, Simons K. (2007) The multiple faces of caveolae. Nat Rev Mol Cell Biol, 8: 185-94.

Pelkmans L, Kartenbeck J, Helenius A. (2001) Caveolar endocytosis of simian virus 40 reveals a new two-step vesicular transport pathway to the ER. Nat Cell Biol, 3: 475-83.

Penheiter SG, Mitchell H, Garamszegi N, Edens M, Dore JJJr, Leof EB. (2002) Internalization-dependent and –independent requirements for trasfotming growth factor beta receptor signaling via the Smad pathway. Mol Cell Biol, 22: 4750-59.

Pietras R, Szego CM. (1977) Specific binding sites for oestrogen at the outer surfaces of isolated endometrial cells. Nature, 265: 69-72

Planas-Silva MD, Waltz PK. (2007) Estrogen promotes reversible epithelial-to-mesenchymal-like transition and collective motility in MCF-7 breast cancer cells. J Steroid Biochem Mol Biol, 104: 11–21.

Razandi M, Oh P, Pedram A, Schnitzer J, Levin ER. (2002) ERs associate with and regulate the production of caveolin: implications for signaling and cellular actions. Mol Endocrinol, 16: 100-115

Razandi M, Pedram A, Greene GL, Levin ER. (1999) Cell membrane and nuclear estrogen receptors derive from a single transcript: studies of ERα and ERβ expressed in CHO cells. Mol Endocrinol, 13: 307-319

Rosenfeld MG, Glass CK. (2001) Coregulator codes of transcriptional regulation by nuclear receptors. J Biol Chem, 276: 36865-36868

Schlegel A, Wang C., Katzenellenbogen BS, Pestell RG, Lisanti MP. (1999) Caveolin-1 potentiates estrogen receptor α (ERα) signaling. J Biol Chem, 274: 33551-33556

Schmidt MW, Houseman A, Ivanov AR, Wolf DA. (2007) Comparative proteomic and transcriptomic profiling of the fission yeast Schizosaccharomyces pombe. Mol Syst Biol, 3: 79

Shi Y, Massagué J. (2003) Mechanisms of TGF-β signaling from cell membrane to the nucleus. Cell, 113: 685-700.

Shook D, Keller R. (2003) Mechanisms, mechanics and function of epithelial-mesenchymal transitions in early development. Mech Dev, 120: 1351-1383.

Simoncini T, Mannella P, Fornari L, Caruso A, Varone G, Genazzani AR. (2004) Genomic and non-genomic effects of estrogens on endothelial cells. Steroids, 69: 537-542

Simpson E, Rubin G, Clyne C, Robertson K, O'Donnell L, Davis S, Jones M. (1999) Local estrogen biosynthesis in males and females. Endocrine-Related Cancer, 6: 131-137

Simpson ER, Rubin G, Clyne C, Robertson K, O'Donnell L, Jones M, Davis S. (2000) The role of local estrogen byosynthesis in males and females. Trends Endocrinol Metab, 11: 184-188

Slot JW, Geuze HJ. (2007) Cryosectioning and immunolabeling. Nat Prot, 2: 2480-2491

Sodek KL, Murphy KJ, Brown TJ, Ringuette MJ. (2012) Cell-cell and cell-matrix dynamics in intraperitoneal cancer metastasis. Cancer Metastasis Rev, 31: 397-414

Song RX, McPherson RA, Adam L, Bao Y, Shupnik M, Kumar R, Santen RJ. (2002) Linkage of rapid estrogen action to MAPK activation by ERα-Shc association and Shc pathway activation. Mol Endocrinol, 16: 116-12

Song RX, Santen RJ. (2006) Membrane initiated estrogen signaling in breast cancer. Biol Reprod, 75: 9-16

Song RX, Zhang Z, Santen RJ. (2005) Estrogen rapid action via protein complex formation involving ERalpha and Src. Trends Endocrinol Metab, 16: 347-353

Sridharan S, Jain K, Basu A. (2011) Regulation of autophagy by kinases. Cancers, 3: 2630-2654

Straub RH. (2007) The complex role of estrogens in inflammation. Endocr Rev, 28: 521–574

Strutz F, Zeisberg M, Ziyadeh FN, Yang CQ, Kalluri R, Müller GA, Neilson EG. (2002) Role of basic fibroblast growth factor-2 in epithelial-mesenchymal transformation. Kidney Int, 61: 1714-28.

Taub N, Teis D, Ebner HL, Hess MW, Huber LA. (2007) Late endosomal traffic of epidermal growth factor receptor ensures spatial and temporal fidelity of mitogen-activated protein kinase signaling. Mol Biol Cell, 18: 4698-4710

Topley N, Jörres A, Luttmann W, Petersen MM, Lang MJ, Thierauch KH, Müller C, Coles GA, Davies M, Williams JD. (1993) Human peritoneal mesothelial cells synthesize interleukin-6: Induction by IL-1β and TNFα. Kidney Int, 43: 226-233

Tsai MJ, O'Malley BW. (1994) Molecular mechanism of action of steroid/thyroid receptor superfamily members. Ann Rev Biochem, 63: 451-486

Tsukazaki T, Chiang TA, Davison AF, Attisano L, Wrana L. (1998) SARA, a FYVE domain protein that recruits Smad2 to the TGF-β receptor. Cell, 95: 779-91.

Vague J, Sardo. (1981) Aromatization of androgens (author's transl) Sem Hop. 57: 1467–1476.

Vanlandingham PA, Ceresa BP. (2009) Rab7 regulates late endocytic trafficking downstream of multivesicular body biogenesis and cargo sequestration. J Biol Chem, 284: 12110-12124

Washburn MP, Koller A, Oshiro G, Ulaszek RR, Plouffe D, Deciu C, Winzeler E, Yates JR. (2003) Protein pathway and complex clustering of correlated mRNA and protein expression analyses in Saccharomyces cerevisiae. Proc Natl Acad Sci USA, 100: 3107–3112

Weibel ER, Kiseler GS, Scherle WF. (1996) Practical stereoloical method for morphometric cytology. J Cell Biol, 30: 23–38

Wrana JL, Attisano L, Wieser R, Ventura F, Massagué J. (1994) Mechanism of activation of TGF-β receptor. Nature, 370: 341-347

Wraner M, Gustaffson JA. (2006) Nongenomic effects of estrogen: why all the uncertainty? Steroids, 71: 91-95

Xiao Z, Latek R, Lodish HF. (2003) An extended bipartite nuclear localization signal in Smad4 is required for its nuclear import and transcriptional activity. Oncogene, 22: 1057-69.

Xie Z, Klionsky DJ. (2007) Autophagosome formation: core machinery and adaptations. Nat Cell Biol, 9: 1102-1109

Xu L, Chen YG, Massagué J. (2000) The nuclear import function of Smad2 is masked by SARA and unmasked by TGFb-dependent phosphorylation. Nat Cell Biol, 2: 559-562.

Yang YH, Chen K, Li B, Chen JW, Zheng XF, Wang YR, Jiang SD, Jiang LS. (2013) Estradiol inhibits osteoblast apoptosis via promotion of autophagy through the ER-ERK-mTOR pathway. Apoptosis, 18: 1363-1375

Ye Y, Xiao Y, Wang W, Yeasley K, Gao JX, Shetuni B, Barsky SH. (2010) ERalpha signaling through slug regulates E-cadherin and EMT. Oncogene, 29: 1451-1462

Zavadil J, Böttinger EP. (2005) TGF-β and epithelial-to-mesenchymal transitions. Oncogene, 24: 5764-5774

Zehorai E, Yao Z, Plotnikov A, Seger R. (2010) The subcellular localization of MEK and ERK-A novel nuclear translocation signal (NTS) paves a way to nucleus. Mol Cell End, 314: 213-220

Zhang S, Fei T, Zhang L, Zhang R, Chen F, Ning Y, Han Y, Feng XH, Meng A, Chen YG. (2007) Smad7 antagonizes transforming growth factor beta signaling in the nucleus by interfering with functional Smad-DNA complex formation. Mol Cell Biol, 27: 4488-99.

Zhang Y, Chang C, Gehling JD, Hemmati-Brivanlou A, Derynck R. (2001) Regulation of Smad degradation and activity by Smurf2, an E3 ubiquitin ligase. Proc Natl Acad Sci U S A, 98: 974-79.

Zuo W, Chen YG. (2009) Specific activation of mitogen-activated protein kinase by transforming growth factor-β receptors in lipid rafts is required for epithelial cell plasticity. Mol Biol Cell, 20: 1020-1029

11.List of publications

List of publications related to the theme of this PhD:

1) Balogh P, Katz S, Kiss AL. (2013): The role of endocytic pathways in TGF-β signaling. Pathol Oncol Res, 19:141-148 (**IF:1,555**)

2) Balogh P, Szabó A, Katz S, Likó I, Patócs A, Kiss AL. (2013) Estrogen receptor alpha is expressed in mesenteric mesothelial cells and is internalized in caveolae upon Freund's adjuvant treatment. PLoS One, (11) p. e79508. 10 p. (**IF: 3,73**)

3) Katz S, Balogh P, Nagy N, Kiss AL. (2012) Epithelial-to-mesenchymal transition induced by Freund's adjuvant treatment in rat mesothelial cells: a morphological and immunocytochemical study. Pathol Oncol Research, 18: 641-649 (**IF: 1,555**)

List of publications not related to the theme of this PhD:

1) Katz S, Balogh P, Kiss AL. (2011) Mesothelial cells can detach from the mesentery and differentiate into macrophage-like cells. APMIS, 119: 782-793 (**IF: 1, 991**)

DOI:10.14753/SE.2015.1712

12.Acknowledgement

I would like to express my thank for the continuous patience of my supervisor *Dr. Anna L. Kiss* who patronized me from the beginning of my medical studies and helped me to succeed as a PhD student by providing a challenging and excellent topic.

Immense thankfullness due to *Prof. Dr. Pál Röhlich* who tirelessly taught me with every of his comments and enhanced the quality of my work.

I also thank to *Prof. Dr. Ágoston Szél* who provided financial support for fellowship and conference attendances and place to complete my research.

I greatly appreciate the financial, professional support and patience of *Dr. Attila Patócs* who facilitated the successfullness of my PhD studies and made a remarkable impact on my scientific view.

I would like to express my gratefulness to *dr. Arnold Szabó* who was always ready to help and taught me with such accuracy for the biochemical techniques.

Special thank to *Dr. István Likó* and *Dr. Nándor Müllner* for their precious help in the biochemical experiments.

I would like to express my gratitude to our assistants Margit Kutasi, Zsuzsanna Újváry, Katalin Lőcsey and Nikoletta Dóczi for their valuable technical help and also thank to all the members of the Department of Human Morphology and Developmental Biology who directly or indirectly but enhanced the effectiveness of my work.

I would like to express my gratefulness for my former chemistry teacher *dr. Jánosné Andó* who implanted in me the seeds of scientific mentality and accuracy in performance.

The patience, the continuous encouragement and support of my *beloved Mother* and sister, *Virág* are inappreciable as well as the motivating and positive energies I have experienced and been given by my closest friends *Katalin* and *Szilveszter*.